Bioactive Materials 6 (2021) 404–419

Contents lists available at ScienceDirect

Bioactive Materials

journal homepage: http://www.keaipublishing.com/biomat

Syntheses and characterization of anti-thrombotic and anti-oxidative Gastrodin-modified polyurethane for vascular tissue engineering

Meng Zheng[a,1], Jiazhi Guo[a,1], Qing Li[a], Jian Yang[b], Yi Han[a], Hongcai Yang[c], Mali Yu[a], Lianmei Zhong[c], Di Lu[a], Limei Li[a,*], Lin Sun[d,**]

[a] Yunnan Key Laboratory of Stem Cell and Regenerative Medicine, Science and Technology Achievement Incubation Center, Kunming Medical University, Kunming, 650500, China
[b] Department of Biomedical Engineering, Materials Research Institute, The Huck Institutes of the Life Sciences, The Pennsylvania State University, University Park, PA, 16802, USA
[c] Department of Neurology, The First Affiliated Hospital, Kunming Medical University, Kunming, 650500, China
[d] Department of Cardiology, The Second Affiliated Hospital, Kunming Medical University, Kunming, 650032, China

ARTICLE INFO

Keywords:
Gastrodin
Polyurethane
Anti-coagulation
Anti-inflammation
Angiogenesis

ABSTRACT

Vascular grafts must avoid negative inflammatory responses and thrombogenesis to prohibit fibrotic deposition immediately upon implantation and promote the regeneration of small diameter blood vessels (< 6 mm inner diameter). Here, polyurethane (PU) elastomers incorporating anti-coagulative and anti-inflammatory Gastrodin were fabricated. The films had inter-connected pores with porosities equal to or greater than 86% and pore sizes ranging from 250 to 400 μm. Incorporation of Gastrodin into PU films resulted in desirable mechanical properties, hydrophilicity, swelling ratios and degradation rates without collapse. The released Gastrodin maintained bioactivity over 21 days as assessed by its anti-oxidative capability. The Gastrodin/PU had better anti-coagulation response (less observable BSA, fibrinogen and platelet adhesion/activation and suppressed clotting in whole blood). Red blood cell compatibility, measured by hemolysis, was greatly improved with 2Gastrodin/PU compared to other Gastrodin/PU groups. Notably, Gastrodin/PU upregulated anti-oxidant factors Nrf2 and HO-1 expression in H_2O_2 treated HUVECs, correlated with decreasing pro-inflammatory cytokines TNF-α and IL-1β in RAW 264.7 cells. Upon implantation in a subcutaneous pocket, PU was encapsulated by an obvious fibrous capsule, concurrent with a large amount of inflammatory cell infiltration, while Gastrodin/PU induced a thinner fibrous capsule, especially 2Gastrodin/PU. Further, enhanced adhesion and proliferation of HUVECs seeded onto films *in vitro* demonstrated that 2Gastrodin/PU could help cell recruitment, as evidenced by rapid host cell infiltration and substantial blood vessel formation *in vivo*. These results indicate that 2Gastrodin/PU has the potential to facilitate blood vessel regeneration, thus providing new insight into the development of clinically effective vascular grafts.

1. Introduction

The replacement of vascular tissue often becomes a clinical necessity due to cardiovascular diseases [1]. Autograft and allograft have been successful in attaining positive outcomes in clinical operations [2]; however, the shortage of donor sites for autograft and the risk of potential disease transmission [3] as well as immune system response of allograft [4] limit their application. Therefore, a series of advanced artificial grafts have been developed and applied clinically, such as expanded polytetrafluoroethylene (ePTFE), Dacron, nylon and polyurethane [5]. Such grafts provide good patency for blood vessels with medium-to large-diameters, but fail for small-diameter blood vessels (SDBVs, inner diameter < 6 mm). When applied in small-diameter vessels that have a much lower blood flow rate, clots can easily form on

Peer review under responsibility of KeAi Communications Co., Ltd.
* Corresponding author.
** Corresponding author.
E-mail addresses: 260763551@qq.com (M. Zheng), 845283279@qq.com (J. Guo), 1847107242@qq.com (Q. Li), jxy30@psu.edu (J. Yang), 2935463101@qq.com (Y. Han), 237461522@qq.com (H. Yang), 1978650544@qq.com (M. Yu), 13888967787@163.com (L. Zhong), 2159164877@qq.com (D. Lu), scullm@163.com (L. Li), sunlinkm@sina.com (L. Sun).
[1] These authors contribute equally to this work.

https://doi.org/10.1016/j.bioactmat.2020.08.008
Received 11 May 2020; Received in revised form 12 August 2020; Accepted 12 August 2020

their luminal surface, causing thrombosis.

Attempts to develop artificial SDBVs actively maintaining graft patency have achieved only modest success [6]. Studies have largely focused on minimizing coagulation through the adhesion of biomolecules that reduce clotting protein activation and the adhesion/activation of platelets [7]. For example, tubes carrying an anticoagulant, such as heparin, inhibit coagulation by targeting either thrombin or platelets; however, heparin-carrying tubes with a small inner diameter may cause hemolysis [8]. The presence of a confluent and healthy layer of endothelial cells on the graft's inner surface is generally a positive indicator of the anti-thrombogenic nature of the graft. Hence, a variety of engineering strategies have been applied to materials in order to induce rapid endothelial cell coverage. Great strides have been made in the area of pre-seeded grafts, where clinical trials have demonstrated remarkable increases in long-term patency of large-diameter grafts [9]. Seeded small-diameter vascular grafts, however, continue to be beset by high failure rates mainly associated with anastomotic hyperplasia (thickening of the tissue at the junction between graft and native vessel due to hyperproliferation of cells and deposition of fibrotic tissue) [10]. To date, no SDBVs (natural, synthetic, or tissue-engineered) have been fully accepted into routine clinical practice, leaving a considerable room for improvement in this field.

Polyurethane (PU) elastomers with high elasticity, low thrombogenicity, and drug loading capacity, have proven to be a promising material class for vascular grafts [11] and stents. Due to their segmented structure, PU elastomers allow fine-tuning of their properties to achieve optimal compliance with biological tissues [12]. PU hyperelasticity can withstand repeated stress, mimicking a native blood vessel subjected to blood flow. Reports by Nafiseh Jirofti et al. [13] suggested that optimized PCL/PU co-electrospun grafts could provide enough mechanical stress to match the native blood vessels. A biodegradable elastomeric PU was designed as a drug-eluting stent coating, such that it was non-thrombogenic and could provide antiproliferative drug release to inhibit smooth muscle cell proliferation [14]. The modification of PU materials, such as hyaluronic acid grafted PU, could facilitate endothelial growth, display vascular-appropriate mechanics and hemocompatibility [15]. Tissue regeneration capability is promoted by the introduction of degradable moieties into the soft and/or hard blocks of PU, which leads to a better long-term performance of the graft [16]. However, degradation is accompanied by a decrease in mechanical properties, as well as inflammatory responses in the vicinity of implants [17].

Unabated inflammation is a cause of failed vascular regeneration of implanted small-diameter vascular grafts in vascular replacement therapies [18]. Recently, increasing evidence supports that modulation of the inflammatory response to biomaterials can play an important role in promoting vascular regeneration [19–21]. The undesirable inflammation caused by the implant itself and injuries following the surgical procedure of implantation have limited further applications. This post-implantation inflammation leads to granulation tissue development, foreign body reactions, and fibrotic capsule formation, all of which impair tissue regeneration and integration between the adjacent tissue and implants and may even cause implant failure [22]. Furthermore, inflammation has been accepted as a key contributor to atherosclerotic calcification [23]. Thus, it is essential to develop strategies to down regulate the inflammatory response of the host and to elicit angiogenesis.

A hydrophilic boundary between implant and host tissue has been used to enhance the biocompatibility of implants [24]. Anti-inflammatory biomolecules have also received significant attention, inhibiting the secretion of mediators such as corticosteroids, and delaying fibroblast capsule formation [25]. A major drawback of these methods is the numerous undesired systemic side effects [26]. Another commonly used method is the induction of angiogenesis based on the use of growth factors [27–29]. Despite its success, this method can overexpose tissues to growth factors, leading to arthritis and tumor formation [30–32]. Furthermore, their bioactive effect can decrease as growth factors are susceptible to biodegradation without any protection in the blood [33]. Hence, alternative strategies that involve simple processing steps to fabricate synthetic materials with not only desirable bulk properties, but also functional amelioration of inflammatory response and thrombogenicity are highly desirable.

Gastrodin, a kind of glucopyranoside with hydroxyl functional groups, plays important roles in treatment of cardiovascular disease [34,35]. It has demonstrated efficacy as a calcium channel blocker and can inhibit intracellular Ca^{2+} overload, raise the blood supply, increase arterial compliance, reduce blood viscosity, and improve microcirculation [35–37]. Gastrodin also exerts an anti-inflammatory effect that is used clinically [38–40]. The aforementioned activity of Gastrodin makes it an attractive small molecule for incorporation into biomaterials that seek to reduce thrombogenicity and inflammatory response. Previous study in our lab demonstrated that Gastrodin can effectively polymerize with PU and improve biocompatibility [41]. However, there has been a dearth of research on introducing Gastrodin into degradable polymers for regenerative engineering applications.

Of particular interest to our work, Gastrodin/PU is polyfunctional. Anti-coagulation and anti-inflammation states are related and thus have to be considered simultaneously in biomaterial design. Such a series of tissue responses are generally used to gauge the biocompatibility of materials. Here, we engineer a porous film based on Gastrodin and PU. In order to enhance degradation to release Gastrodin, we introduced poly (ethylene glycol) (PEG) and L-lysine ethyl ester (Lys·OEt) for PU syntheses. Hydrophilic PEG is capable of promoting degradation [42,43], while its high chain mobility provides good resistance against the adsorption of plasma proteins and platelet adhesion under physiological conditions. The long term objective of this study is to delineate the potential of Gastrodin loaded vascular grafts (Fig. S2) to accelerate vascular tissue regeneration and reinforce its clinical suitability. The major hypothesis underlying our efforts is that Gastrodin can be used to simultaneously: (1) improve scaffold surface and mechanical properties, and (2) be effectively released from the biodegradable PU matrix. We tested these hypotheses through physico-chemical characterization of the effect of varying Gastrodin doses on films. The effect of the films on coagulation was evaluated by hemocompatibility analysis as well as protein and platelet adhesion/activation. Subsequently, *in vitro* cell culture and *in vivo* subcutaneous implantation of the film were also addressed in terms of inflammatory response and angiogenesis. The unique and favorable biological responses endowed the films with significant potential for vascular tissue regeneration.

2. Materials and methods

2.1. Fabrication of Gastrodin/PU films

2.1.1. Reagents

Gastrodin (purity > 99.0%) was purchased from Kunming Pharmaceutical Co. Ltd., China. Poly (Ɛ-caprolactone)2000 (PCL2000), isophorone diisocyanate (IPDI) and Lysine ethyl ester dihydrochloride (Lys·OEt-2HCl) were purchased from Aladdin Co. Ltd., China. Acetonitrile was purchased from Shanghai Thermo Fisher Scientific, China. Poly (ethylene glycol)400 (PEG400) was purchased from Chengdu Kelong Chemical Reagent Technology (China). Tianjin Fengchuan Chemical Reagent Technology (China) was the source of other chemicals of AR grade. NaCl particles were ground into a fine powder and then sifted through sieves of 300 mesh diameter (< 50 μm).

2.1.2. Synthesis of Gastrodin/PU

PU materials were fabricated by *in situ* polymerization according to our previous research [41]. Briefly, 24.00 g of PCL2000, 1.2 g of PEG400 and 7.80 g of IPDI were mixed in a 250 mL three-necked flask under nitrogen atmosphere heated at 70 °C with thorough stirring for

Table 1
The composition of films.

Sample	IPDI(g)	PCL2000(g)	PEG400(g)	The ratio of NCO:OH in the prepolymer	Lys·OEt-2HCl(g)	Gastrodin content (wt%)
PU	7.8	24	1.2	2.3:1	3.7	–
1Gastrodin/PU	7.8	24	1.2	2.3:1	3.7	1
2Gastrodin/PU	7.8	24	1.2	2.3:1	3.7	2
5Gastrodin/PU	7.8	24	1.2	2.3:1	3.7	5

4 h to obtain the prepolymer. Subsequently, 3.70 g of Lys·OEt-2HCl was employed as a chain extender to extend the prepolymer. After stirring for 2 h, Gastrodin (0%, 1%, 2%, 5%, shown in Table 1) was added. The resultant mixture was cured at 90 °C for 18 h.

2.1.3. Preparation of porous Gastrodin/PU films

Porous films were fabricated by a solvent casting/salt-leaching process. Gastrodin/PU materials were dissolved in 1,4-dioxane with sodium chloride salt in a 1:2 ratio of material to salt (by weight). The slurry was mixed thoroughly to become a viscous paste, and was then cast into Teflon molds. After air drying for 24 h to eliminate solvent, the salt in the scaffold was leached out by immersion in deionized water under vacuum for 48 h to form porous films. The dried film was removed from the Teflon plate to yield Gastrodin/PU films with an average thickness of about 2 mm.

2.2. Characterization of Gastrodin/PU films

2.2.1. Morphology observation

The microstructure of films was observed by scanning electron microscopy (SEM, FEI Quanta-200, Switzerland) at an accelerating voltage of 10 kV. All samples were mounted onto SEM specimen stubs and sputter-coated with a 7 nm layer of gold for contrast in vacuum.

2.2.2. FT-IR and NMR analysis

The chemical structure of films was confirmed by Fourier transform-infrared spectra (FT-IR, Nicoletis10, Thermo fisher scientific, USA) recorded in the transmission mode from wavenumbers 4000 to 400 cm^{-1}. The characteristic functional groups of films were further verified by ^1H nuclear magnetic resonance (^1H NMR, DRX500, Bruker advance) using a 600 MHz spectrometer.

2.2.3. Mechanical test

Mechanical properties were measured similar to our previous report using a uniaxial load test machine (AG-I 250, SHIMADZU, Japan). Rectangular specimens (100 × 10 × 2 mm^3) were tested in quintuplicate. Samples were pulled at a speed of 200 mm/min and strained to rupture. Tensile strength, Tensile modulus and Peak stress were then calculated.

2.2.4. Contact angle

Water contact angles indicating the wettability of materials were measured by drop shape analysis (DSA 100, Kruss, Germany). 3 μL of deionized water was dropped on the sample surfaces. At least five measurements were performed at different locations and the results averaged.

2.2.5. Swelling

The swelling behavior of Gastrodin/PU films was evaluated according to ASTM D570-98 [44]. Dried strips (1 × 1 cm^2, n = 5) were weighed and then soaked in phosphate buffered saline (PBS) at 37 °C. At predetermined time periods, specimens were removed, blotted by a filter paper to remove adsorbed water and weighed. The swelling ratio was calculated from Equation. (1):

$$Swelling\ ratio(\%) = [(Ww - Wd)/Wd] \times 100\% \quad (1)$$

Where W_w and W_d represent the weights of the wet and dried specimens, respectively.

2.2.6. Degradation study

Degradation of specimens was performed in 200 U/mL lipase solution (Lipase (porcine pancreas), Shanghai yuanye Bio-Technology Co., Ltd, China) at 37 °C, shaking at 100 rpm. For each study, ~0.3 g of specimens (Ø 13 mm × 2 mm, n = 5) were placed into capped tubes containing 5 mL of the degradation buffer with solution change twice per week. Detailed procedures are provided in supplementary information (SI).

2.3. Hemocompatibility in vitro

Detailed procedures of platelet adhesion, bovine serum albumin (BSA) and fibrinogen adsorption, hemolysis test, quantification of whole blood clotting time, activated partial thromboplastic time (APTT) and prothrombin time (PT) assays are provided in SI.

2.4. Cytocompatibility of films in vitro

Human umbilical vein endothelial cells (HUVECs) were obtained from the Bei Na Chuanglian Biotechnology (BNCC, Wuhan, China). Following sterilization with γ-ray irradiation with 15 kGy, the disks (Ø 13 mm × 2 mm) were incubated overnight in 24-well plates using RPMI-1640 media (Corning, USA) supplemented with 10% fetal bovine serum (Gibco, USA), 1% penicillin-streptomycin (HyClone, USA) in a humidified incubator (37 °C, 5% CO_2), and then seeded with HUVECs (5 × 10^4 cells/well), changing the media every 2 days.

2.4.1. Cell viability

The viability of HUVECs growing on the films was observed with fluorescence microscopy (IX73, OLYMPUS, Japan) on day 1, 3 and 5. Before observation, cells were labeled with the live/dead reagent (LIVE/DEAD Viability/Cytotoxicity Kit, Life Technologies, USA). Cell proliferation was also evaluated via CCK8 assay (Cell Counting kit-8, Dojindo Molecular Technologies, Japan) with a multilabel counter (Spectra Max 190, Molecular Devices Corporation) at 450 nm.

2.4.2. Anti-oxidant ability of films

The anti-oxidant ability of films cultured with H_2O_2 treated HUVECs was assessed by reverse transcription and quantitative polymerase chain reaction (RT-qPCR) to measure HO-1 and Nrf2 expression. After culture for 3 days, the samples were exposed to 1 mM H_2O_2 for 2 h. Detailed procedures are provided in SI.

2.5. In vitro anti-inflammatory response

Anti-inflammatory response of films was assessed using RAW 264.7 cells (leukemia cells in mouse macrophage cell line). Briefly, cells (1 × 10^6 cells/mL) were seeded onto sterilized films in 24-well plates in a humidified incubator (37 °C, 5% CO_2) using complete Dulbecco's Modified Eagle's medium (DMEM, Gibco, USA) media. In order to assess the anti-inflammatory activity, RAW 264.7 cells were stimulated with 10 ng/mL LPS (Lipopolysaccharide, Solarbio, China) compared with the blank control (tissue culture plastic). After 18 h, cells were collected to

analyze TNF-α and IL-1β expression by RT-qPCR. The morphology of cells was evaluated using SEM after rinsed with PBS, dehydrated through graded ethanol, and dried in a vacuum. Viability of cells on films were also observed after labeled with Live/Dead reagent.

2.6. Inflammatory responses in vivo

Fifteen Sprague-Dawley rats (male, 150–200 g) were employed in subcutaneous implantation in accordance with the protocol approved by the Experimental Animal Center of Kunming Medical University in compliance with all the guidelines and regulations. Rats were randomly divided into PU, 1Gastrodin/PU, 2Gastrodin/PU and 5Gastrodin/PU groups. Each sterilized disc specimen (Ø 13 mm × 2 mm) was placed into the dorsal subcutaneous pocket symmetrically per rat (n = 3, Fig. S3), and harvested for analysis after 2 and 6 weeks. The implants with surrounding tissue were retrieved and fixed with 4% paraformaldehyde in PBS for 7 days. Once dehydration was done using gradient ethanol, each sample was cleaned with xylene, embedded in paraffin wax, and cut into 5 μm thick sections. After sections were deparaffinized and rehydrated, staining (H&E, Masson, TNF-α, IL-1β, CD31 and VE-Cadherin) was performed on the sections followed by imaging under optical microscope.

2.7. Statistical analysis

All statistical analyses were performed using the statistical software SPSS 10.0. Data were reported as means ± standard deviations (SD). A statistically significant difference was accepted at $P < 0.05$.

3. Results

3.1. Physico-chemical properties of the films

3.1.1. Structure

A PU elastomer incorporating Gastrodin was successfully synthesized in this study (Fig. 1A). Chemical structure of Gastrodin/PU was characterized by FT-IR and ^{1}H NMR. As shown in Fig. 1B, the stretching peaks at around 2864 and 2942 cm^{-1} were assigned to CH_3 and CH_2. The ether stretch at 1095 cm^{-1} belonged to the -OCH_2CH_2- repeating unit of PEG. The ester bending vibration at 1191 cm^{-1} identified the C-O-C of PCL [45]. A strong peak at 1725 cm^{-1} belonged to the carbonyl (C=O) stretching of urethane (OCONH) groups of PU. The band at 1529 cm^{-1} was associated with -NH in the PU, whereas this peak was not detected in the spectra of PCL, PEG and Gastrodin. The strong -OH peak in Gastrodin was significantly reduced in PU, indicating its role in polymerization, as demonstrated in our previous reports [41]. These observations support the formation of Gastrodin/PU elastomer.

^{1}H NMR spectrum further confirmed the formation of Gastrodin/PU (Fig. 1C and D). Peaks at 1.36 (h), 1.63 (g, i), 2.34 (j) and 4.05 (f) ppm were assigned to methylene protons of -$(CH_2)_3$-, -$OCCH_2$-, and -CH_2OOC- in PCL units, respectively. The sharp single peak at 3.66 ppm (k) was attributed to the methylene protons of homosequences of the PEG oxyethylene units. The very weak peak at 4.3 ppm (l) was attributed to the methylene proton of PEG end units [46,47]. The characteristic peaks at 0.9–1.0 ppm (d, e) of IPDI [48], could be clearly identified. The protons close to the urethane functional groups were also observed at 3.86–3.88 ppm (b) [49]. In addition, the peak at 7.01 ppm (a, c) was attributed to the Gastrodin [50], which was absent in the PU. These results confirm the reaction between Gastrodin and IPDI.

3.1.2. Morphology

The SEM images revealed inter-connected and open pores with porosities equal to or greater than 86% (Fig. S4). Pore sizes ranged from 250 to 400 μm throughout the volume of the film (Fig. 1E-G. Of note, the microstructure was not obviously changed after adding Gastrodin at different contents in the PU matrix.

3.1.3. Mechanical properties

The mechanical properties were increased with increasing Gastrodin content. As can be seen (Fig. 2), the tensile modulus of 5Gastrodin/PU (82.386 ± 8.542 MPa), 2Gastrodin/PU (30.832 ± 7.541 MPa), and 1Gastrodin/PU (14.560 ± 6.272 MPa) were significantly higher than that of the PU group (10.463 ± 2.769 MPa). 2Gastrodin/PU had the highest break stress (53.603 ± 5.056 MPa) with the highest tensile strength (3.953 ± 0.036 MPa), while PU had the least tensile stress at break (22.413 ± 2.037 MPa) and tensile strength (1.377 ± 0.169 MPa). Both the tensile strength and modulus of samples were higher than 882 ± 133 kPa and 264 kPa of native small diameter arteries [51].

3.1.4. Contact angle and swelling

The surface wettability of films was determined by water contact angle measurement (Fig. 3A and B). It could be seen clearly that the water contact angles of samples were gradually decreased with increased Gastrodin content. When the content of Gastrodin was 5 wt%, the water contact angle decreased to approximately 0° followed by 2Gastrodin/PU with increased time. The similar effect of Gastrodin content on water uptake capacity was reflected in Fig. 3C.

3.1.5. Degradation study

As can be observed in Fig. 4(A, B-E), pure PU and 5Gastrodin/PU films showed significant rupture and conglutination after 5 weeks of degradation. These samples flattened and collapsed, losing the previous cylindrical shape. 1Gastrodin/PU and 2Gastrodin/PU showed a slight fracture without conglutination and enlarged pore size. Film degradation curves in terms of mass loss are shown in Fig. 4F. PU with or without Gastrodin exhibited progressive mass loss during the 5-week degradation period. There was a significantly higher degradation rate for 2Gastrodin/PU compared with other Gastrodin/PU groups ($p < 0.001$), while PU was slowest. The change of pH values is also presented in Fig. 4G, and increased dramatically with time, becoming close to 6.0 after 5 weeks.

The Gastrodin release profile (Fig. 4H) showed no obvious initial burst over a period of 21 days. Consistent with degradation results, 2Gastrodin/PU films had a considerably higher release of Gastrodin than 5Gastrodin/PU, while 1Gastrodin/PU released the least. Antioxidant activity of released Gastrodin was quantified by DPPH free radical scavenging. Fig. 4I presented a higher scavenging rate for Gastrodin/PU films than PU, indicating that incorporated Gastrodin contributed to a higher anti-oxidant activity. The released media from 2Gastrodin/PU showed significant ($p < 0.001$) anti-oxidation over the first 3 days.

3.2. In vitro hemocompatibility

Fig. 5(A-H) showed the *in vitro* platelet distribution and morphology on film surfaces. A large number of platelets adhered on the PU surface and presented pseudopodia, suggesting the activated phenotype. In contrast, a rounded shape was seen on the few platelets adhered to the Gastrodin/PU, while the 2Gastrodin/PU surface presented the smallest platelet number and spreading area compared with the other surfaces. Quantitative characterization of BSA (Fig. 5I) and fibrinogen (Fig. 5J) adsorption on each surface was consistent with the visible platelet images.

Hemolysis rate was Gastrodin content-dependent (Fig. 5K). The hemolysis rate of PU was much higher than the Gastrodin/PU groups, reaching 1.33%. 2Gastrodin/PU had the slowest hemolysis rate, suggesting that optimizing Gastrodin in PU could effectively improve hemocompatibility.

The response of films to whole blood was assessed by clotting time. As shown in Fig. 5L, all films can prolong the value in a Gastrodin

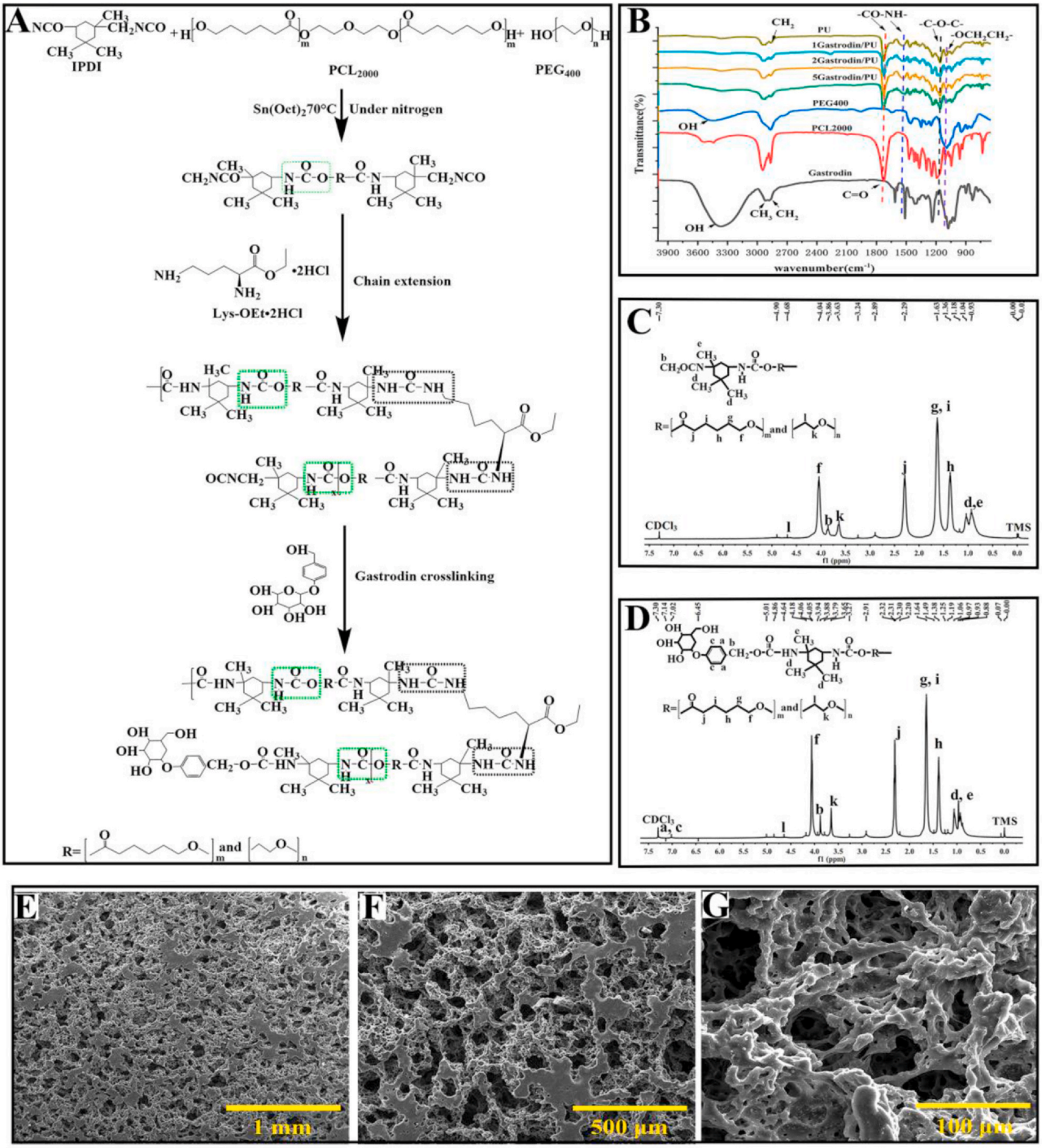

Fig. 1. Chemical structure and morphology of Gastrodin/PU films. (A) Synthesis schematic of Gastrodin/PU polymers. (B) FTIR spectra of Gastrodin, PCL2000, PEG400 and Gastrodin/PU films. (C, D) ^{1}H NMR spectrum of PU (C) and 5Gastrodin/PU (D). (E–G) SEM images of porous microstructure of 2Gastrodin/PU.

content- and time-dependent manner, and 2Gastrodin/PU had greater impact than the other groups, which suggested it had a greater influence on the coagulation factors in plasma. There was no significant difference in the degree of clotting among PU, 1Gastrodin/PU and 5Gastrodin/PU until 35 min. Blood incubated with the PU had a higher degree of clotting at 45 min. Impact on plasma coagulation time was likely associated with surface properties, as was the case for platelet activation.

Blood clotting disorders resulting from a deficiency of coagulation factor are specifically diagnosed using the APTT and PT assays, which are conventional clinical tests of coagulation and can be used to measure the effect of Gastrodin on the activity of coagulation factors. As shown in Fig. 5(M, N), Gastrodin/PU groups could all prolong the APTT and PT values in a content dependent manner, with greater impact on APTT. Particularly, Gastrodin content of 2 wt% increased APTT and PT values obviously compared to the control.

3.3. Anti-oxidant activity

Gastrodin-induced HO-1 and Nrf2 expression was involved in protecting H_2O_2-induced oxidative injury in HUVECs. As observed in Fig. 6, both HO-1 and Nrf2 expression for Gastrodin/PU showed a

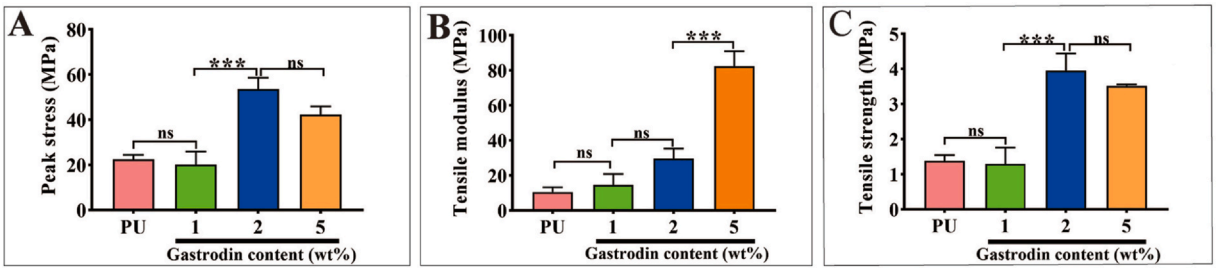

Fig. 2. Effect of Gastrodin content on the mechanical properties of Gastrodin/PU films. (A) Peak stress, (B) Tensile modulus and (C) Tensile strength. (Error bars represent standard deviation from the mean (n = 5). ***$p < 0.001$; *$p < 0.05$; ns: no significant difference.).

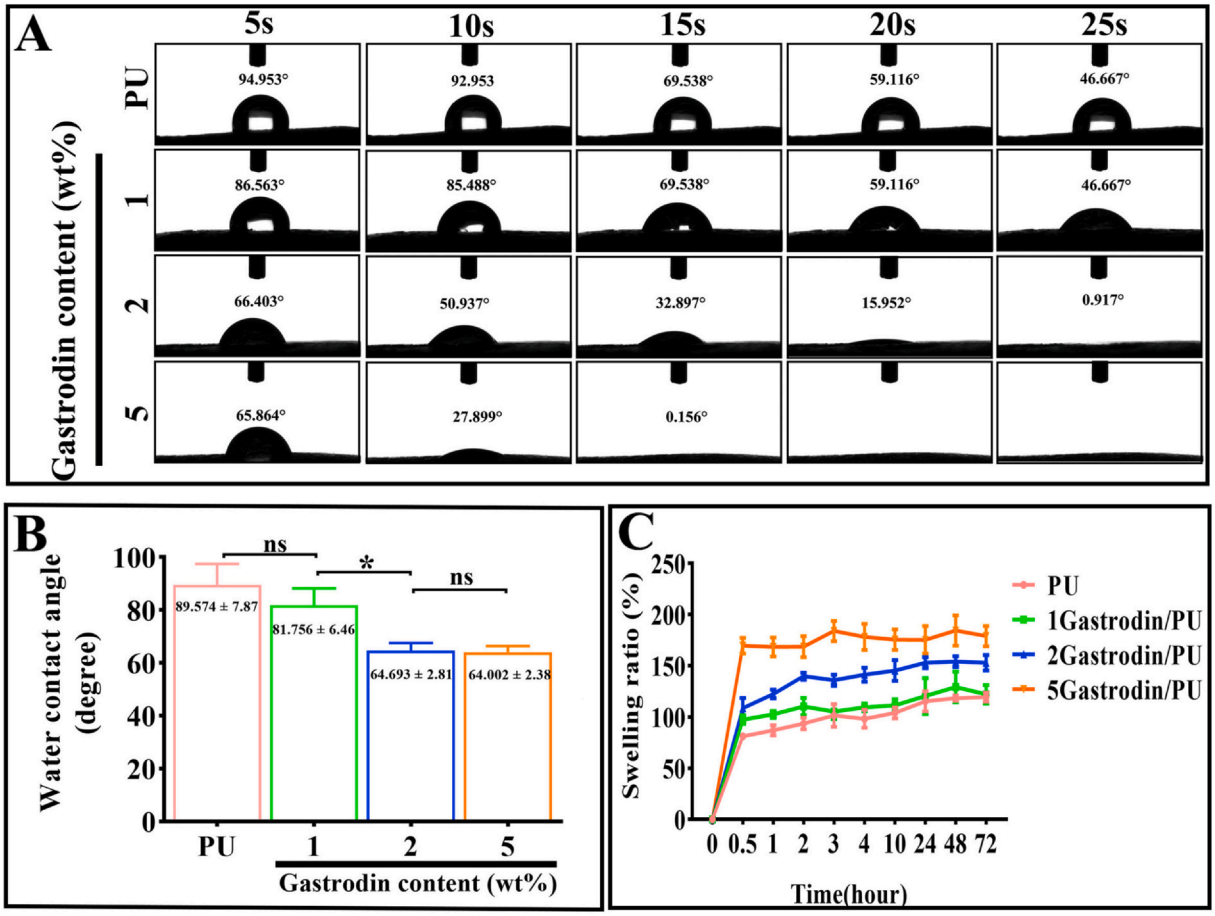

Fig. 3. Effect of Gastrodin content on the hydrophilicity of Gastrodin/PU films. (A) Water contact angles of various Gastrodin/PU films at desired time points (5, 10, 15, 20 and 25 s). (B) Initial contact angles. (C) The swelling ratio of specimens. (Error bars represent standard deviation from the mean (n = 5). *$p < 0.05$; ns: no significant difference.).

significant increase compared to PU after 3 days. Notably, 2Gastrodin/PU had the strongest capacity to induce Nrf2 and HO-1 expression, presenting a similar pattern to DPPH analysis.

3.4. Anti-inflammation properties

As shown in Fig. 7, RAW 264.7 cells on the control and films (K-T) exhibited a round morphology. No severe cytotoxic effect of samples on the macrophage. Inflammatory conditions were induced through incubation of RAW 264.7 cells with LPS (A-J). Cells on control (A, F) appeared activated flat and many synaptic structures morphology, while cells on the films (B-E, G-J) presented round morphology, indicating the suppression of inflammatory state.

We further investigated the anti-inflammation function of the films by assessing the TNF-α and IL-1β mRNA expression of macrophages. Fig. 7(U, V) shows that samples groups could significantly reduce TNF-α and IL-1β expression compared with the positive LPS group. 2Gastrodin/PU presented the lowest level, indicating suppression of macrophages activation. Films did not trigger undesired inflammatory response and were compatible with macrophages.

3.5. In vitro cell viability

HUVECs were cultured on the films to investigate the cell adhesion and proliferation through CCK-8 and fluorescence staining. Results showed that cells could adhere and grow on the surface of each film (Fig. 8) on day 3, but the cell density was higher for Gastrodin/PU groups than PU. Cells covered most of the area of the 2Gastrodin/PU surface and exhibited a typical fibroblastic morphology of HUVECs having a higher degree of spreading. In PU and 1Gastrodin/PU groups,

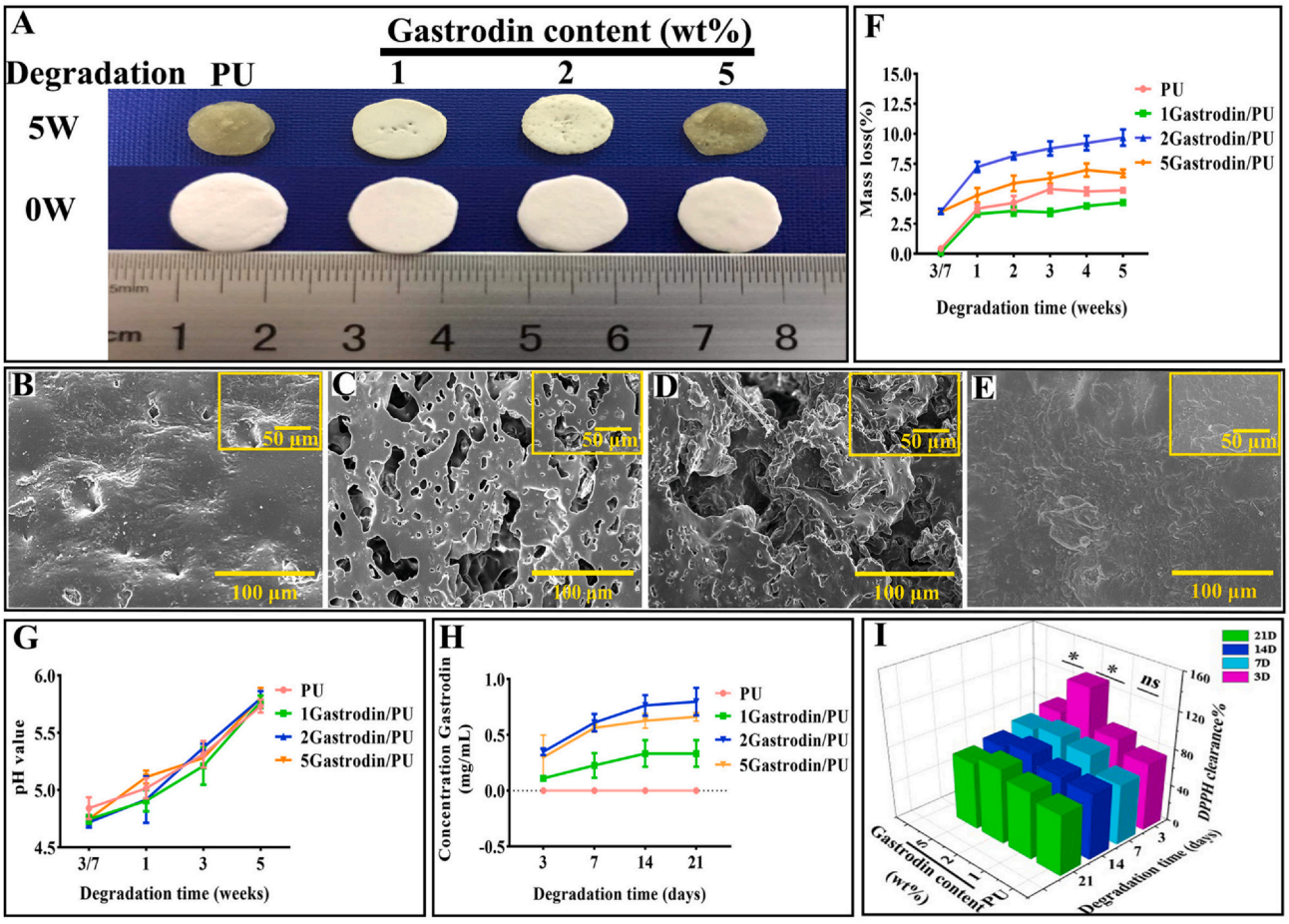

Fig. 4. *In vitro* degradation studies of Gastrodin/PU films in lipase solution. (A) Digital photos and (B–E) SEM morphology of the films after 5 weeks of degradation: (B) PU, (C) 1Gastrodin/PU, (D) 2Gastrodin/PU, (E) 5Gastrodin/PU. (F) Effect of Gastrodin on mass loss. (G)The pH of media and (H) Gastrodin release profiles from films. (I) DPPH assay of free radical inhibition. (Error bars represent standard deviation from the mean (n = 5). ***$p < 0.001$; *$p < 0.05$).

a few dead cells were obvious, displaying a small spherical or narrow shape, a typical non-adherent and non-spreading morphology of HUVECs. This difference was also reflected in the cell viability from CCK-8. While all groups displayed a significant increase in the cell viability on day 5 of culture when compared to day 1 and 3, the viability of Gastrodin/PU groups was found to progressively increase unlike PU, which showed moderate growth. Notably, cells on the 2Gastrodin/PU film exhibited the highest proliferation rate and formed capillary-like networks, suggesting its potential for vascular grafts.

3.6. Host response to films in subcutaneous implantation

To evaluate the host response to the films, PU with or without Gastrodin was separately implanted subcutaneously in SD rats. Following a 2-week implantation, the tissues surrounding the implanted films were distinctly different. Histological analysis (Masson's trichrome staining, Fig. 9) showed that host cells penetrated into the pores of porous films and inflammatory cells were found adjacent to the PU implant surface during the acute inflammation stage. In contrast, only a few inflammatory cells accumulated within Gastrodin modified films. Moreover, the collagenous fibrous capsules surrounding the PU (0.898 ± 0.028), 1Gastrodin/PU (0.546 ± 0.093) and 5Gastrodin/PU (0.993 ± 0.061) were visually much thicker in comparison with 2Gastrodin/PU (0.401 ± 0.087), as verified by quantitative examination. At 6-weeks (Fig. 10), there were marked differences in the inflammatory response to the four films. The thickness of fibrous capsules decreased, especially for Gastrodin/PU. The expression of pro-inflammatory cytokines IL-1β and TNF-α were obviously attenuated for Gastrodin/PU (Fig. S5). The decreasing inflammatory cells have also been found at the interface of tissue and films for 2Gastrodin/PU from H&E staining (Fig. 11). The results suggest that optimal Gastrodin loading may incite a weaker inflammatory response.

To further explore the effect of Gastrodin/PU on vessel generation, vascular endothelial cadherin (VE-Cadherin) and platelet EC adhesion molecule (CD31) immunostaining was performed (Fig. 12, Fig. S6). At week 2 postoperatively, there was a notably higher intensity for the 2Gastrodin/PU group than other Gastrodin/PU groups. As time progressed, large amounts of vessels grew around 2Gastrodin/PU with more CD31 expression at 6 weeks. The quantitative analysis showed that the fluorescent intensity of CD31 and VE-Cadherin was consistent with the visible images (Fig. 12D-F). The images from H&E staining also revealed more blood vessels and red cells within the 2Gastrodin/PU (Fig. 11). Overall, the data suggests that the 2Gastrodin/PU can reduce inflammatory response and enhance angiogenesis.

4. Discussion

Vascular grafts should have good blood compatibility and avoid triggering inflammation, as well as facilitating vessel generation. Foreign surfaces may activate blood cells leading to uncontrolled thrombotic and inflammatory responses that ultimately result in implant failure [52]. Limiting thrombogenicity of polymers for small-diameter vascular grafting is thus of critical importance. Many approaches have been utilized to improve the SDBVs blood compatibility, including surface modification [53–55], polymer composition modification [14,56], nitric oxide release [57–59] and drug release [60,61].

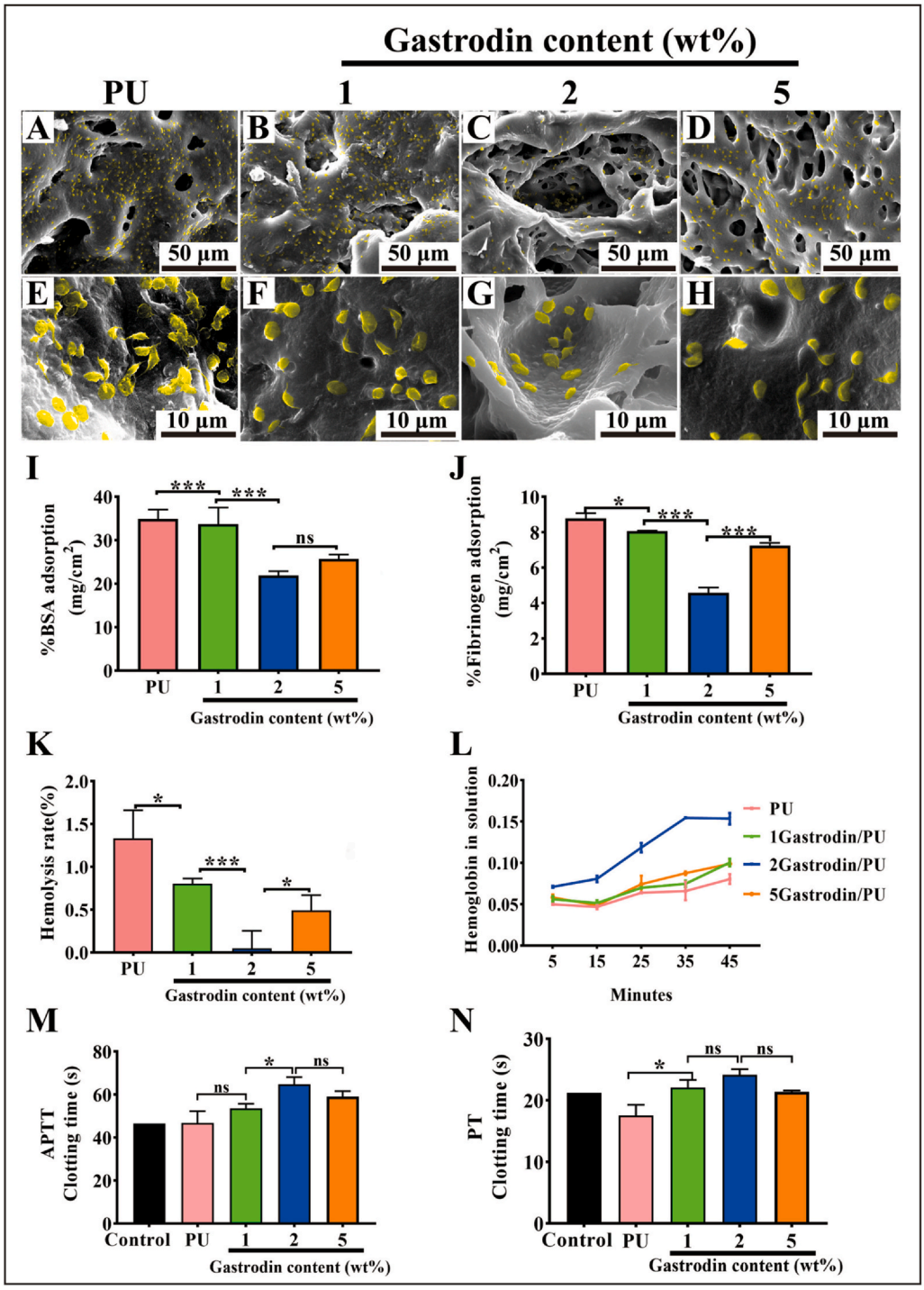

Fig. 5. *In vitro* hemocompatibility analysis of Gastrodin/PU films. (A–H) SEM images of SD rat platelet-rich plasma (PRP) incubated on Gastrodin/PU films: (A, E) PU, (B, F) 1Gastrodin/PU, (C, G) 2Gastrodin/PU, (D, H) 5Gastrodin/PU. (I) BSA adsorption on various films. (J) Fibrinogen adsorption on various films. (K) Hemolysis rate of whole blood incubated with various films. (L) The effect of Gastrodin content in the PU matrix on thrombus formation in whole blood at 5, 15, 25, 35 and 45 min. APTT (M) and PT (N) of plasma coagulation in the presence of various films. (Error bars represent standard deviation from the mean (n = 5). ***$p < 0.001$; **$p < 0.01$; *$p < 0.05$; ns: no significant difference.).

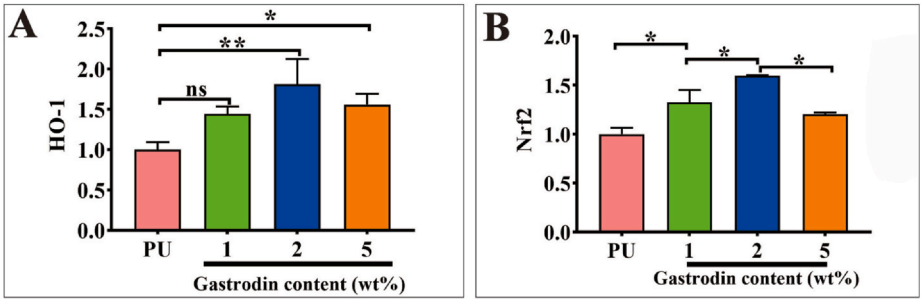

Fig. 6. Efficacy on anti-oxidant activity of the Gastrodin/PU films *in vitro*. The quantification of HO-1 (A) and Nrf2 (B) expression in H_2O_2 treated HUVEC cells when seeded onto various films as determined by RT-qPCR. (Error bars represent standard deviation from the mean (n = 3). ***$p < 0.001$; **$p < 0.01$; *$p < 0.05$; ns: no significant difference.).

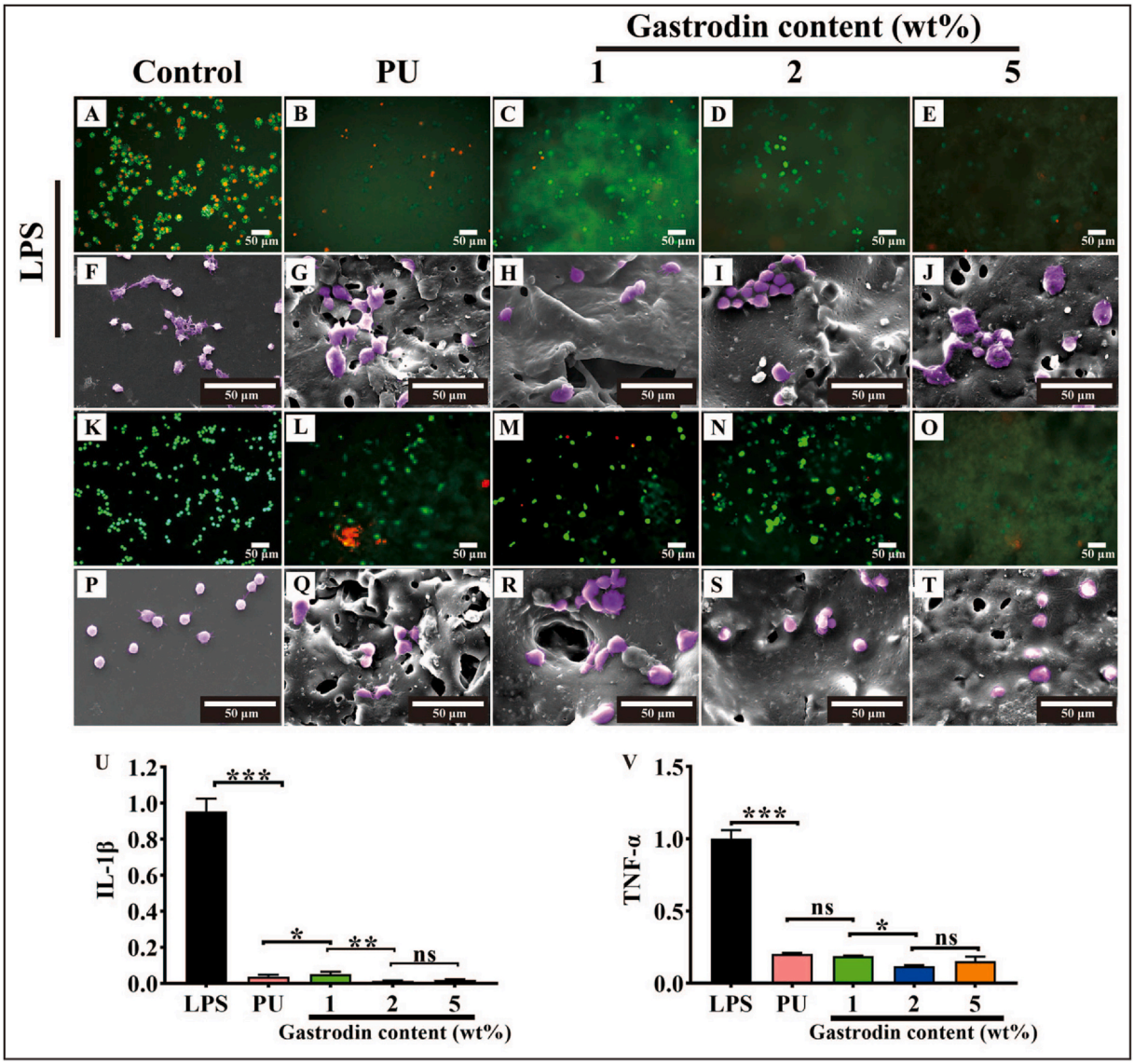

Fig. 7. Efficacy on anti-inflammation properties of the Gastrodin/PU films *in vitro*. (A–J) Fluorescence (A–E) and SEM (F–J) images of Raw 264.7 on films activated with LPS for 18 h: (A, F) Positive control (LPS treated), (B, G) PU, (C, H) 1Gastrodin/PU, (D, I) 2Gastrodin/PU, (E, J) 5Gastrodin/PU. Fluorescence (K-O) and SEM (P–T) images of Raw 264.7 on films: (K, P) Blank control, (L, Q) PU, (M, R) 1Gastrodin/PU, (N, S) 2Gastrodin/PU, (O, T) 5Gastrodin/PU. The pro-inflammatory cytokine IL-1β (U) and TNF-α (V) expression in Raw 264.7 cells when seeded onto various films as determined by RT-qPCR. (Error bars represent standard deviation from the mean (n = 3). ***$p < 0.001$; **$p < 0.01$; *$p < 0.05$; ns: no significant difference.).

Of these strategies, the drug release approach is an easy way to improve the biofunctions of polymers. PU is a well-accepted bio/hemocompatibility implant material used in prostheses [62–64] including vascular grafts, restenosis at the microvascular level can still occur. Punnakitikashem et al. [65] found that the dipyridamole -loaded scaffolds reduced thrombogenicity compared to the PU urea alone. Its disadvantage was adverse to human aortic endothelial cells accommodation. Hong et al. [56] reported that phosphorycholine-bearing polymer coated or blended PUs significantly limited initial thrombotic occlusion. However, the phosphorycholine was difficult to permeate throughout the primary structural PU, which may lead to the erosion of the (non-degradable) phosphorycholine-bearing polymer and loss of the anti-thrombogenic effectiveness during chronic use. Here, anti-thrombotic and anti-oxidative Gastrodin-modified PU for vascular tissue engineering was successively developed (Fig. 1A).

Films had inter-connected pores with porosities of 86% or greater and pore sizes ranging from 250 to 400 μm (Fig. 1E–G), capable of facilitating vascular ingrowth (pore sizes greater than 250 μm have been considered to be essential for *in vivo* vascularization) [66]. The incorporated Gastrodin in PU resulted in enhanced mechanical properties. Gastrodin, with multiple hydroxyl groups, increased polar-polar interactions with urethane and hydrogen bonding within its molecular chains [67]. Enhanced mechanical properties potentially allow both 2Gastrodin/PU and 5Gastrodin/PU to resist mechanical forces and blood pressures without collapsing during *in vitro* and *in vivo* conditions. However, 2Gastrodin/PU maintained its porous structure without collapse after 5 weeks in enzyme solution, while 5Gastrodin/PU completely deformed (Fig.4A, B-E). Biodegradable/remodeling of grafts is deemed an attractive feature in tissue regeneration [16]. Degradation caused not only large pores and surface areas, which promoted cell infiltration, but also effective biomolecule release from the polymer matrix [68]. Accelerated degradation is ascribed to increased hydrophilicity and swelling ratio as the content of hydrophilic Gastrodin increased. PDI, an indicator of molecular weight distribution that is correlated with degradation [69,70], was also higher in 2Gastrodin/PU (Table S1). More importantly, the release profile of 2Gastrodin/PU was

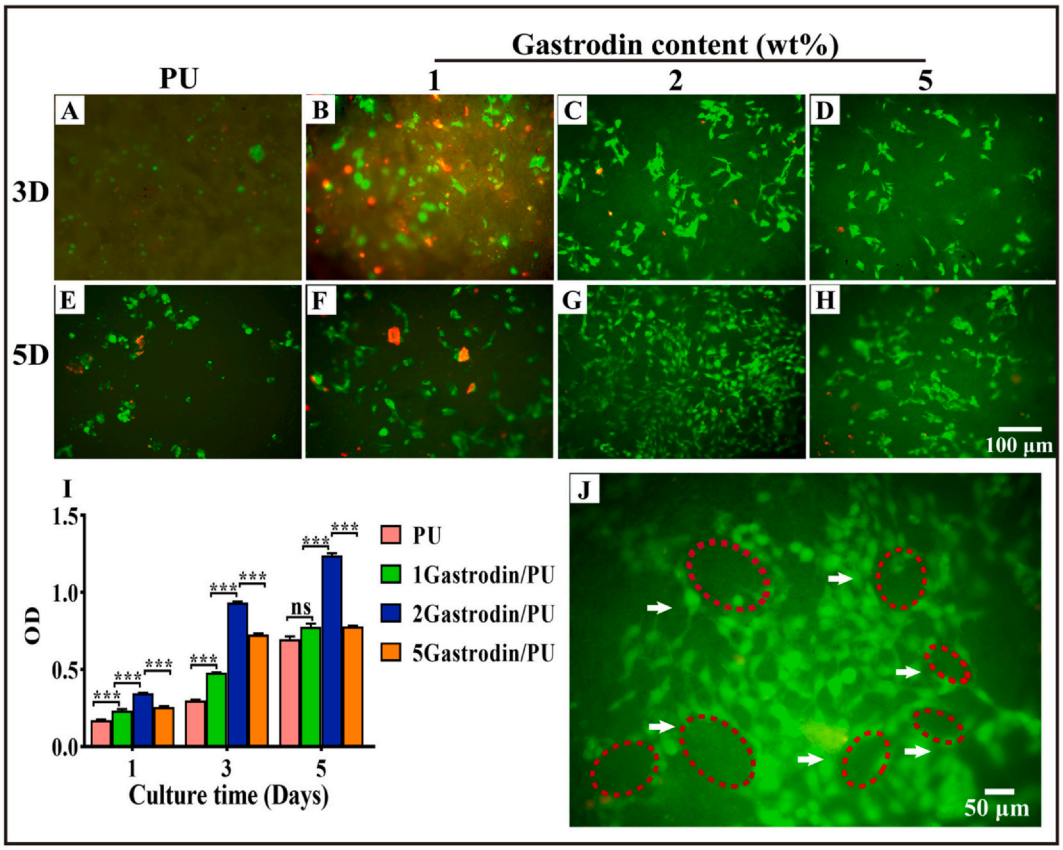

Fig. 8. Cell adhesion and proliferation on Gastrodin/PU films *in vitro*. (A–H) Fluorescence images of HUVECs on films after 3 and 5 days: (A, E) PU, (B, F) 1Gastrodin/PU, (C, G) 2Gastrodin/PU, (D, H) 5Gastrodin/PU. Live cells are stained green, dead cells are stained red. (I) CCK-8 assay for proliferation of HUVECs cultured with films after 1, 3, 5 days. (J) High magnification of 2Gastrodin/PU sample showed capillary-like networks in the surface of films. (Error bars represent standard deviation from the mean (n = 3). ***$p < 0.001$.).

highly efficient and successfully maintained over a period of up to 21 days compared to 5Gastrodin/PU, most likely resulting from a higher diffusion rate due to the elevated degradation. Sustained release of 2Gastrodin/PU without a high initial burst would benefit anti-coagulant and anti-inflammatory response as well as functional regulation during the vascular remodeling process.

When materials come in contact with blood, protein is first absorbed instantaneously onto the surface and deformed, then a large number of platelet adhesion and serious distortion leads to the formation of a thrombus due to triggering of inflammation and coagulation [71]. Therefore, a study on protein adsorption, platelet adhesion, whole blood clotting time and hemolysis rate to evaluate the anti-coagulant properties of the material was conducted. BSA (Fig. 5I) and fibrinogen adsorption (Fig. 5J) on the Gastrodin/PU film surfaces was significantly lower when compared to pure PU, contributing to their potential to produce a hydrated surface, forming a hydration barrier which imitated the natural environment encountered by plasma proteins. As was noted, increased hydrophilicity was thought to inhibit nonspecific protein adsorption [72–77]. When examining the platelet-rich plasma contacted surfaces by SEM (Fig. 5A–H), the images showed few platelets which maintained a discoidal shape with a small spreading area on the Gastrodin/PU, whereas many aggregated and deformed platelets were found on PU, indicating that coagulation was attenuated by loaded Gastrodin. Hemolysis is also an important indicator of the outcome of vascular graft implantation as broken erythrocytes release adenosine diphosphate (ADP), which activates the platelets through a guanosine triphosphate (GTP) binding protein. This ADP-platelet interaction may lead to a change in the shape of platelets and a decline in cyclic adenosine phosphate (cAMP) formation, causing platelet activation and further accelerating clotting and thrombus formation [78,79]. We assessed hemolysis on each sample. Hemolysis rates were lower than the lowest permissible limits of the USA FDA (1%) and Council of Europe (0.8%) for biomaterials, suggesting that they are highly compatible with blood, with barely any induction of hemolysis for 2Gastrodin/PU. The hydrophilic and hydrophobic property of a biomaterial may affect the morphology of red blood cells which is associated with hemolysis. Yang et al. [80] inferred that the hydrophobic surface was able to affect the cytoskeleton of the red blood cells, thereby causing the morphological alternation of red blood cells and leading to hemolysis. Wang et al. [81] reported that hydrophilic PU/PEG hybrid scaffold surfaces showed much lower hemolysis rate compared with the blank PU. Our Gastrodin modified PU with the ability to establish hydrogen bonding interaction with water molecules, thus reduced hemolysis.

In addition, prolonged clotting times correlate with improved thromboresistance of the biomaterial [82]. PEG, an effective molecule at reducing bioadhesion (protein adsorption, platelet deposition) as a surface modifying agent [83,84], was employed to synthesis PU. Particularly, Gastrodin has anti-coagulant activity and the mechanism mainly involves its interference with the knob-to-hole interactions between fibrin molecules, thereby effectively inhibiting occurrence of hemolysis, decreasing formation of clots and the risk of thrombosis [37]. The blood coagulation cascade includes two major pathways, the intrinsic and the extrinsic pathway [85], assessed by APTT and PT, respectively. The extrinsic pathway is responsible for hemostatic control and response to vascular injury whereas the intrinsic pathway has a slight physiological significance under normal conditions. The intrinsic pathway triggered by blood-material interaction is an important factor causing poor hemocompatibility of biomaterials. The common range of APTT and PT in humans is respectively 20–50 s and 11–30 s [86]. Our study concluded that APTT results showed a statistically significant

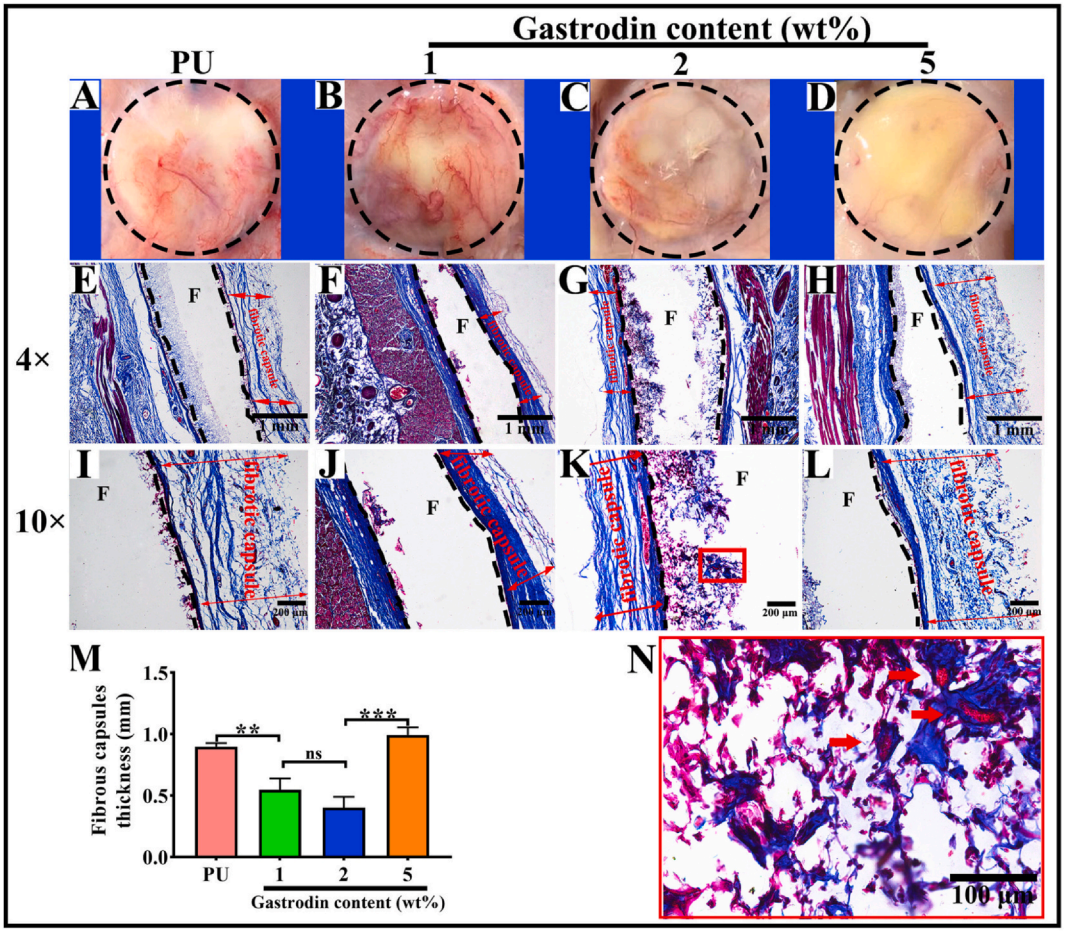

Fig. 9. Histological analysis of host response to the Gastrodin/PU films following 2-week subcutaneous implantation. Retrieved tissue samples (A–D) and Masson's Trichrome-stained histological sections (E–L) of PU (A, E, I), 1Gastrodin/PU (B, F, J), 2Gastrodin/PU (C, G, K) and 5Gastrodin/PU (D, H, L). (M) Analysis of the thickness of fibrotic capsules surrounding the implants. (N) Representative high magnification images of the stained 2Gastrodin/PU sample. "F" denotes films and the dashed lines mark the tissue-material implant interface. Arrows indicate blood vessels; two-way red arrows mark the span of the fibrotic capsule at the film-tissue interface. (Error bars represent standard deviation from the mean (n = 3). $***p < 0.001$, $**p < 0.01$; $*p < 0.05$; ns: no significant difference.).

increase in plasma clotting time (PU (46.817 ± 5.514 s), 1Gastrodin/PU (53.563 ± 2.194 s), 2Gastrodin/PU (64.853 ± 3.274 s), 5Gastrodin/PU (59.127 ± 2.500 s)), suggesting the enhanced anti-coagulation nature of Gastrodin/PU (> 50 s) by delaying intrinsic pathways. However, there was little effect on the extrinsic route of blood coagulation. A steep upward trend for 2Gastrodin/PU illustrated its superior anti-coagulant property, thus reducing the possibility of blood coagulation and thrombus formation. Importantly, Gastrodin released from films is a calcium channel blocker and can inhibit intracellular Ca^{2+} overload, raise the blood supply, increase arterial compliance, reduce blood viscosity, and improve microcirculation [37,40]. Reports by Liu et al. also verified Gastrodin plays a positive role in anti-coagulation [37].

Thrombosis and coagulation also readily occur due to the lack of an EC layer or the failure to properly reendothelialize after implantation. The presence of a confluent and healthy layer of endothelial cells on the material's surface is generally a positive indicator of the anti-thrombogenic nature [8]. Porous films helped HUVECs attachment and spreading. The observed divergence between PU and Gastrodin/PU groups is likely related to the hydrophilicity and stimulation effect of Gastrodin [41]. Cells spread effectively and a confluent endothelial layer was formed on 2Gastrodin/PU (Fig. 8C and G). The higher Gastrodin release from 2Gastrodin/PU facilitated cell proliferation. This effect of Gastrodin in a dose-dependent manner was also evidenced by Lin et al. [87]. These findings suggest a strong influence from optimal Gastrodin content in PU, as in this condition the anti-coagulant was largely enhanced.

Inflammation is another important issue for the implantation of vascular grafts [7,18]. Failure to resolve the foreign inflammatory response typically leads to granulation (formation of connective tissue) and fibrotic capsule formation around the implant [88]. Moreover, inflammation has been generally associated with pro-oxidative environments and cardiovascular diseases. At the sites of implantation several factors (e.g., healing response of the diseased artery, biomaterial-induced inflammatory response, and effects of the surgical wound) could contribute to the accumulation of reactive oxygen species (ROS) and thus induce high levels of oxidative stress, which is one of the most important contributors to destruction of the anti-oxidant defense system [89–91]. Once oxidative stress has been restrained, inflammation can be suppressed. Gastrodin has also been shown to reduce ROS of ECs induced with H_2O_2, and up-regulate HO-1 and Nrf2 protein expression to protect H_2O_2-induced oxidative injury [92]. Therefore, incorporation of Gastrodin into PU in this study has been developed to enhance anti-oxidant properties. Our results demonstrate that Gastrodin released from materials maintained its inherent anti-oxidant activity (Fig. 4I), and radical scavenging ability was positively correlated with the release rate of Gastrodin. Additionally, Gastrodin/PU groups had obvious free radical scavenging activity when compared to PU, and thus effectively up-regulated HO-1 and Nrf2 expressions against oxidative stress to protect HUVECs from oxidative apoptosis (Fig. 6). Specially, there was a clear indication of strong anti-oxidant activity in 2Gastrodin/PU.

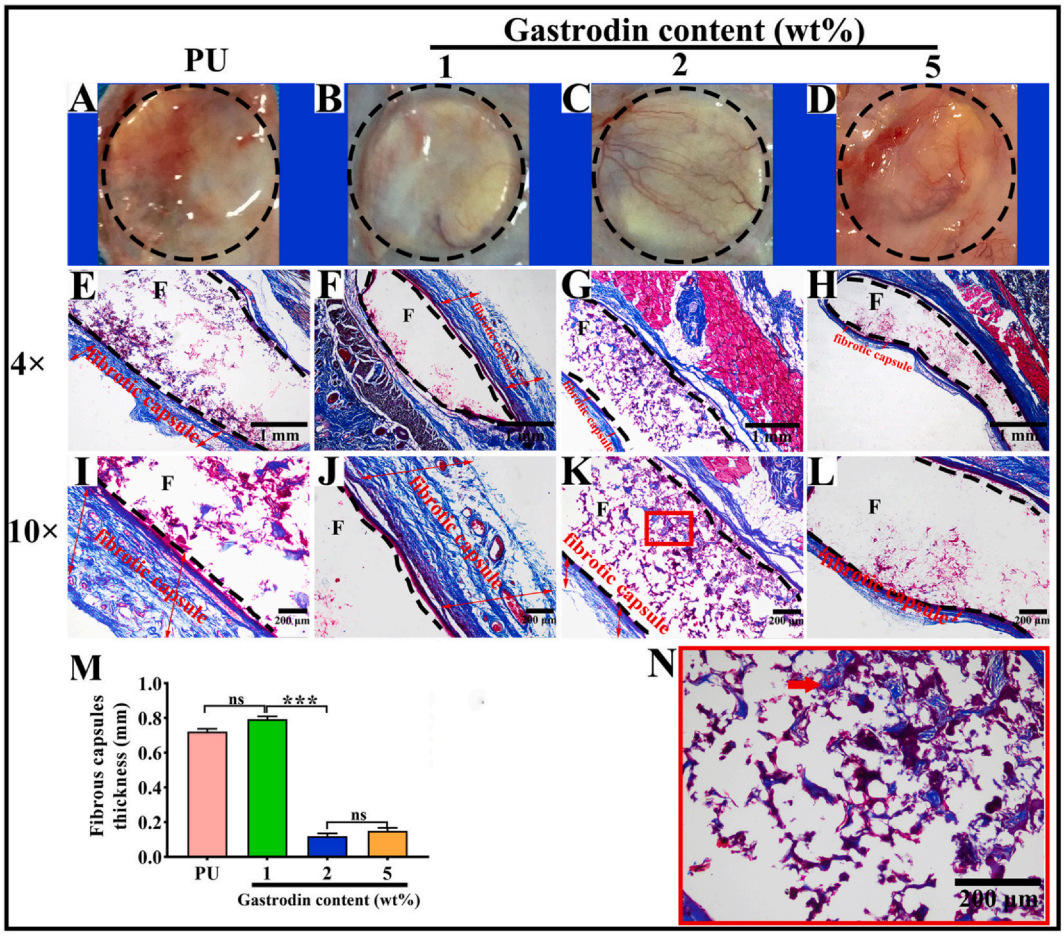

Fig. 10. Histological analysis of host response to the Gastrodin/PU films following 6-week subcutaneous implantation. Retrieved tissue samples (A–D) and Masson's Trichrome-stained histological sections (E–L) of PU (A, E, I), 1Gastrodin/PU (B, F, J), 2Gastrodin/PU (C, G, K) and 5Gastrodin/PU (D, H, L). (M) Analysis of the thickness of fibrotic capsules surrounding the implants. (N) Representative high magnification images of the stained 2Gastrodin/PU sample. "F" denotes films and the dashed lines mark the tissue-material implant interface. Arrows indicate blood vessels; two-way red arrows mark the span of the fibrotic capsule at the film-tissue interface. (Error bars represent standard deviation from the mean (n = 3). $^{***}p < 0.001$, $^{**}p < 0.01$; $^{*}p < 0.05$; ns: no significant difference.).

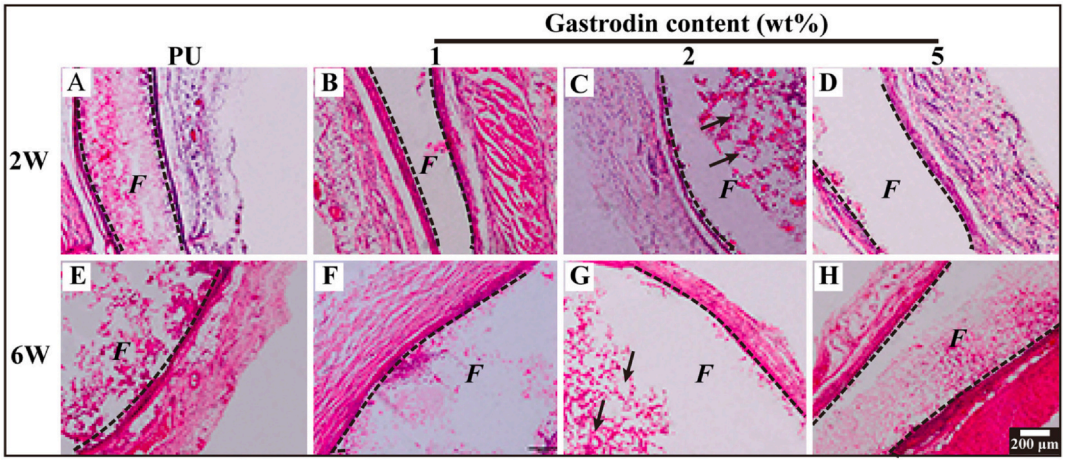

Fig. 11. Histological analysis of inflammatory response and angiogenesis within the Gastrodin/PU films. H&E-stained histological sections of PU (A, E), 1Gastrodin/PU (B, F), 2Gastrodin/PU (C, G) and 5Gastrodin/PU (D, H) following 2-week (A–D) and 6-week (E–H) subcutaneous implantation. "F" denotes films and the dashed lines mark the tissue-material implant interface. Black arrows indicate blood vessels.

The inflammatory activation of macrophages is normally associated to morphological changes. Pro-inflammatory macrophages exhibit flat and many synaptic structures morphology accompanied with an enlargement of the spreading area [93,94]. When cultured with films, cells kept their original round shape without being activated, especially for Gastrodin/PU (Fig. 7 (H-J)), compared to control (Fig. 7 F). Further, the inflammatory response induced by Gastrodin/PU was evaluated in terms of specific pro-inflammatory cytokines released from adherent RAW 264.7 cells (TNF-α and IL-1β). Inflammation and blood coagulation are intimately linked; with inflammation promoting the

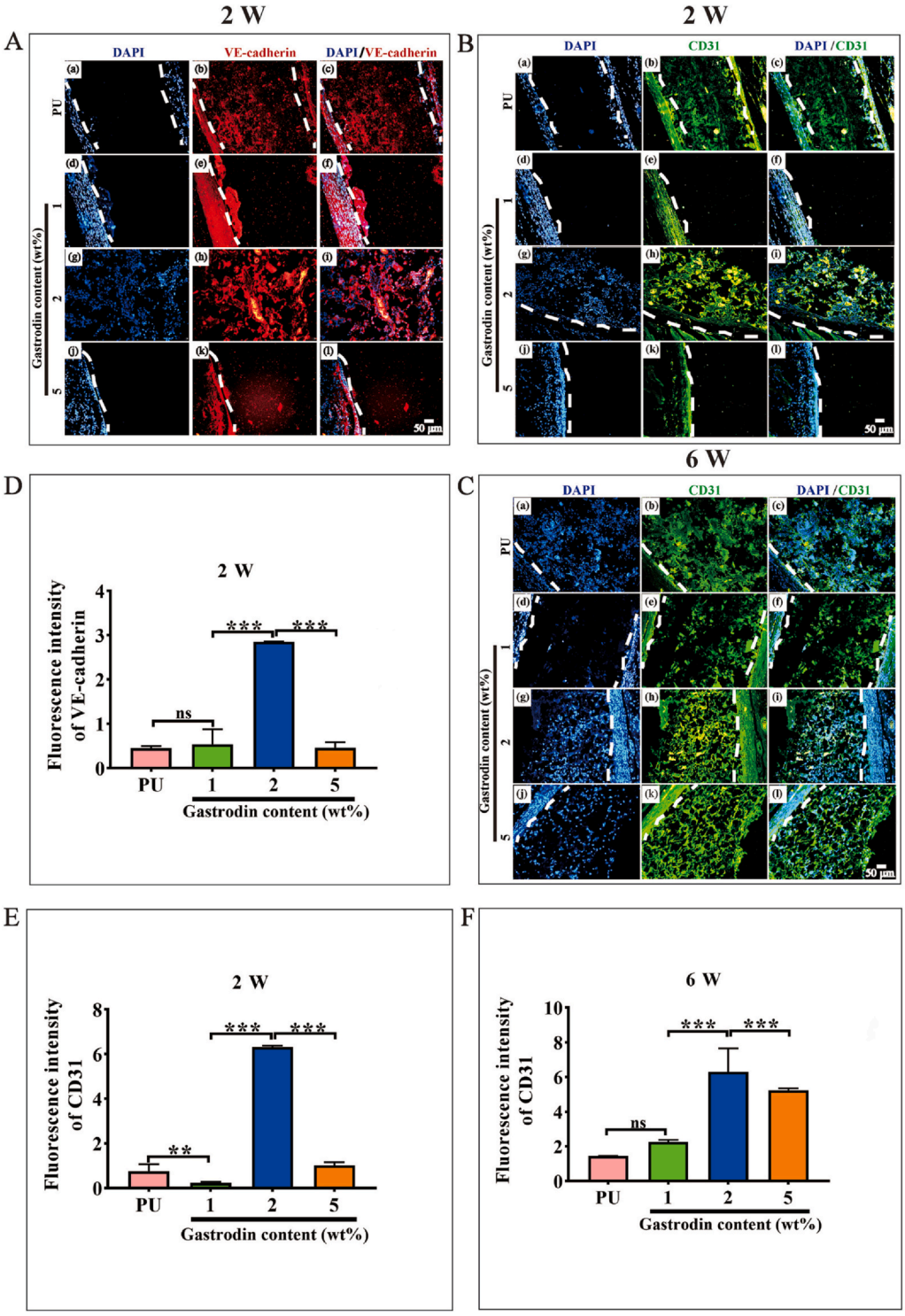

Fig. 12. Angiogenesis within the Gastrodin/PU films in subcutaneous implantation. (A) Immunofluorescence staining of VE-Cadherin at 2 weeks; (B, C) Immunofluorescence staining of CD31 at 2 weeks (B) and 6 weeks (C): (a–c) PU, (d–f) 1Gastrodin/PU, (g–i) 2Gastrodin/PU and (j–l) 5Gastrodin/PU. VE-Cadherin was stained red, CD31 was stained green and cell nuclei was stained blue with DAPI. White dashed lines indicate the interface between the film and tissue interface. (D–F) Quantitative analysis (fluorescence intensity) of VE-Cadherin expression at 2 weeks (D), CD31 expression at 2 weeks (E) and 6 weeks (F). (Error bars represent standard deviation from the mean (n = 3). ***$p < 0.001$, **$p < 0.01$; ns: no significant difference.).

development of cardiovascular disease and tipping the hemostatic balance towards thrombosis and DIC (Disseminated intravascular coagulation) [95,96]. At the molecular level, TNF-α and IL-1β are major players in inflammation-induced activation of the coagulation system [97]. As expected, the levels of TNF-α and IL-1β secreted by macrophages were significantly down-regulated after exposure to 2Gastrodin/PU. These results aligned with our observations in anti-oxidant testing. *In vitro* 2Gastrodin/PU maximally limits their activation resulting in a modification of their oxidant and inflammatory activity. Yang et al. [98] reported that Gastrodin significantly attenuated the inflammatory response in cardiomyocytes as increased Gastrodin content, which could be up to 10 mM. Our *in vivo* studies further suggested that 2Gastrodin/PU induced a thinner fibrotic capsule manifested by loose collagen fibers (Figs. 9 and 10 (G, K)), fewer infiltrated inflammatory cells (Fig. 11(C, G)) and decreased pro-inflammatory cytokine IL-1β and TNF-α expression (Fig. S5(i)).

An ideal replacement vascular graft would result in functional remodeling that leads to the formation of neo-vessels. As the first step toward this, we evaluated adhesion and proliferation of HUVECs seeded onto films. 2Gastrodin/PU had cell spreading over a large area (Fig. 8C, G). Cell adhesion onto a biomaterial surface is of particular importance for subsequent events [88]. Following subcutaneous implantation,

more cells from the host tissue were found to infiltrate into pores of 2Gastrodin/PU than other groups (Fig. 9K). Moreover, abundant collagen fibers were visual by Masson's trichrome staining at the 6-week time point (Fig. 10K).

Vascularization of implanted grafts may also be very helpful for cellularization and neotissue formation. Cells infiltrating into thick grafts face nutrient- and metabolic starvation if there is a paucity of blood vessels or capillary-like networks in the scaffold material [99–101]. Therefore, strategies focused on enhancing neovascularization are of considerable importance. Lin et al. [102] reported that Gastrodin can enhance vascularization in regenerated tissue and facilitate wound healing. Accordingly, 2Gastrodin/PU film promoted the regeneration of significant numbers of blood vessels after 6 weeks (Fig. 12, Fig. S6), manifested by positive CD31 and VE-Cadherin expression. The secretion of CD31 and VE-Cadherin from EC is related to the angiogenesis of EC and is well known to not only participate in the maintenance of normal EC phenotype activity (migration and proliferation), but also wound healing, neo-vascularization, and angiogenesis [100,103]. These results reveal that our developed films can promote direct secretion of angiogenetic factors and can induce angiogenesis. The combined anti-coagulation, anti-inflammation and angiogenesis effects of 2Gastrodin/PU make it an excellent candidate for vascular grafting in future studies.

5. Conclusions

The present study fabricated Gastrodin/PU scaffolds prepared by a solvent casting/salt-leaching process, aiming at better anti-coagulation and anti-inflammatory performance for small-diameter vascular biomaterials. The inter-connected pores, mechanical properties, degradation rate and Gastrodin release testing confirmed the 2Gastrodin/PU sample was distinct in comparison with other Gastrodin containing samples, which further led to their distinct bioactivity. 2Gastrodin/PU proved to be anti-hemolytic, with minimal adhesion/activation of BSA, fibrinogen and platelets, and prolonged coagulation times, suggesting attenuation of coagulation. It also elicited a better anti-inflammatory response in terms of up-regulated anti-oxidant factor Nrf2 and HO-1 expressions, as well as decreasing pro-inflammatory cytokine (TNF-α and IL-1β) levels *in vitro*, perhaps owing to improved material hydrophilicity and sustained Gastrodin release. *In vivo* subcutaneous implantation resulted in minimal inflammatory cell infiltration and formation of thinner fibrotic capsules. HUVECs culture results indicated that the 2Gastrodin/PU significantly enhanced cell growth and coverage, suggesting better recruitment of host cells. When implanted into a subcutaneous pocket, collagen fibers and neo-vessels were visible within scaffolds. 2Gastrodin/PU exhibited both anti-coagulation and anti-inflammatory properties, justifying its application as a blood-contacting anti-thrombotic material. However, further studies at *in vivo* level are needed to ascertain clinical applicability.

CRediT authorship contribution statement

Meng Zheng: Investigation, Formal analysis, Visualization. **Jiazhi Guo:** Data curation. **Qing Li:** Formal analysis. **Jian Yang:** Writing - review & editing. **Yi Han:** Formal analysis. **Hongcai Yang:** Investigation, Visualization. **Mali Yu:** Formal analysis. **Lianmei Zhong:** Resources. **Di Lu:** Validation. **Limei Li:** Conceptualization, Writing - original draft. **Lin Sun:** Conceptualization, Supervision.

Declaration of competing interest

The authors declare that they have no known competing financial interests or personal relationships that could have appeared to influence the work reported in this paper.

Acknowledgments

This research was supported by the National Natural Science Foundation of China (81760087/31760292/81860326/81560050), and the Department of Science and Technology of Yunnan Province of China (2017FA035/2017FE467(-008)/2018FE001(-137)/2018FE001(-165)/2018FE001(-125)/2018IA048/2019ZF011-2), Major Program of Kunming Science and Technology Innovation Center (2019-1-N-25318000003568), Program for Innovative Research Team (in Science and Technology) in University of Yunnan Province (IRTSTYN).

Appendix A. Supplementary data

Supplementary data to this article can be found online at https://doi.org/10.1016/j.bioactmat.2020.08.008.

References

[1] D. Prabhakaran, S. Anand, D. Watkins, Cardiovascular, respiratory, and related disorders: key messages from Disease Control Priorities, The Lancet 391 (10126) (2018) 1224–1236, https://doi.org/10.1016/S0140-6736(17)32471-6 third ed..
[2] Y. Yao, J. Wang, Y. Cui, R. Xu, Z. Wang, J. Zhang, K. Wang, Y. Li, Q. Zhao, D. Kong, Effect of sustained heparin release from PCL/chitosan hybrid small-diameter vascular grafts on anti-thrombogenic property and endothelialization, Acta Biomater. 10 (6) (2014) 2739–2749, https://doi.org/10.1016/j.actbio.2014.02.042.
[3] D.D. Swartz, S.T. Andreadis, Animal models for vascular tissue-engineering, Curr. Opin. Biotechnol. 24 (5) (2013) 916–925, https://doi.org/10.1016/j.copbio.2013.05.005.
[4] H. Du, L. Tao, W. Wang, D. Liu, Q. Zhang, P. Sun, S. Yang, C. He, Enhanced biocompatibility of poly(l-lactide-co-epsilon-caprolactone) electrospun vascular grafts via self-assembly modification, Mater. Sci. Eng. C 100 (2019) 845–854, https://doi.org/10.1016/j.msec.2019.03.063.
[5] S. Asadpour, H. Yeganeh, J. Ai, H. Ghanbari, A novel polyurethane modified with biomacromolecules for small-diameter vascular graft applications, J. Mater. Sci. 53 (14) (2018) 9913–9927, https://doi.org/10.1007/s10853-018-2321-5.
[6] D. Seifu, A. Purnama, K. Mequanint, D. Mantovani, Small-diameter vascular tissue engineering, Nat. Rev. Cardiol. 10 (2013), https://doi.org/10.1038/nrcardio.2013.77.
[7] J.T. Patterson, T. Gilliland, M.W. Maxfield, S. Church, Y. Naito, T. Shinoka, C.K. Breuer, Tissue-engineered vascular grafts for use in the treatment of congenital heart disease: from the bench to the clinic and back again, Regen. Med. 7 (3) (2012) 409–419, https://doi.org/10.2217/rme.12.12.
[8] Y. Tamada, Sulfation of silk fibroin by sulfuric acid and anticoagulant activity, J. Appl. Polym. Sci. 87 (14) (2003) 2377–2382, https://doi.org/10.1002/app.12022.
[9] Y. Hong, S.-H. Ye, A. Nieponice, L. Soletti, D.A. Vorp, W.R. Wagner, A small diameter, fibrous vascular conduit generated from a poly(ester urethane)urea and phospholipid polymer blend, Biomaterials 30 (13) (2009) 2457–2467, https://doi.org/10.1016/j.biomaterials.2009.01.013.
[10] R.Y. Kannan, H.J. Salacinski, P.E. Butler, G. Hamilton, A.M. Seifalian, Current status of prosthetic bypass grafts: a review, J. Biomed. Mater. Res. B Appl. Biomater. 74B (1) (2005) 570–581, https://doi.org/10.1002/jbm.b.30247.
[11] L. Xue, H.P. Greisler, Biomaterials in the development and future of vascular grafts, J. Vasc. Surg. 37 (2) (2003) 472–480, https://doi.org/10.1067/mva.2003.88.
[12] R. Song, M. Murphy, C. Li, K. Ting, C. Soo, Z. Zheng, Current development of biodegradable polymeric materials for biomedical applications, Drug Des. Dev. Ther. 12 (2018) 3117–3145, https://doi.org/10.2147/DDDT.S165440.
[13] N. Jirofti, D. Mohebbi-Kalhori, A. Samimi, A. Hadjizadeh, G.H. Kazemzadeh, Small-diameter vascular graft using co-electrospun composite PCL/PU nanofibers, Biomed. Mater. 13 (5) (2018) 055014, , https://doi.org/10.1088/1748-605x/aad4b5.
[14] Y. Hong, S.H. Ye, A.L. Pelinescu, W.R. Wagner, Synthesis, characterization, and paclitaxel release from a biodegradable, elastomeric, poly(ester urethane)urea bearing phosphorylcholine groups for reduced thrombogenicity, Biomacromolecules 13 (11) (2012) 3686–3694, https://doi.org/10.1021/bm301158j.
[15] T.W. Chuang, K.S. Masters, Regulation of polyurethane hemocompatibility and endothelialization by tethered hyaluronic acid oligosaccharides, Biomaterials 30 (29) (2009) 5341–5351, https://doi.org/10.1016/j.biomaterials.2009.06.029.
[16] W. Wu, R.A. Allen, Y. Wang, Fast-degrading elastomer enables rapid remodeling of a cell-free synthetic graft into a neoartery, Nat. Med. 18 (7) (2012) 1148–1153, https://doi.org/10.1038/nm.2821.
[17] L. Pinchuk, A review of the biostability and carcinogenicity of polyurethanes in medicine and the new generation of 'biostable' polyurethanes, J. Biomater. Sci. Polym. Ed. 6 (3) (1994) 225–267, https://doi.org/10.1163/156856294x00347.
[18] S. de Valence, J.-C. Tille, D. Mugnai, W. Mrowczynski, R. Gurny, M. Möller, B.H. Walpoth, Long term performance of polycaprolactone vascular grafts in a rat abdominal aorta replacement model, Biomaterials 33 (1) (2012) 38–47, https://doi.org/10.1016/j.biomaterials.2011.09.024.

[19] C. Davis, J. Fischer, K. Ley, I.J. Sarembock, The role of inflammation in vascular injury and repair, J. Thromb. Haemostasis 1 (8) (2003) 1699–1709, https://doi.org/10.1046/j.1538-7836.2003.00292.x.

[20] S.A. Eming, M. Hammerschmidt, T. Krieg, A. Roers, Interrelation of immunity and tissue repair or regeneration, Semin. Cell Dev. Biol. 20 (5) (2009) 517–527, https://doi.org/10.1016/j.semcdb.2009.04.009.

[21] A. Nurden, Platelets, Inflammation and tissue regeneration, Thromb. Haemostasis 105 (Suppl 1) (2011) S13–S33, https://doi.org/10.1160/THS10-11-0720.

[22] J.M. Anderson, A. Rodriguez, D.T. Chang, Foreign body reaction to biomaterials, Semin. Immunol. 20 (2) (2008) 86–100, https://doi.org/10.1016/j.smim.2007.11.004.

[23] L. Bessueille, D. Magne, Inflammation: a culprit for vascular calcification in atherosclerosis and diabetes, Cell. Mol. Life Sci. 72 (13) (2015) 2475–2489, https://doi.org/10.1007/s00018-015-1876-4.

[24] M. Nune, U.M. Krishnan, S. Sethuraman, PLGA nanofibers blended with designer self-assembling peptides for peripheral neural regeneration, Mater. Sci. Eng. C 62 (2016) 329–337, https://doi.org/10.1016/j.msec.2016.01.057.

[25] I.A. Halaby, S.P. Lyden, M.G. Davies, E. Roztocil, L.J. Salamone, A.I. Brooks, R.M. Green, H.J. Federoff, W.J. Bowers, Glucocorticoid-regulated VEGF expression in ischemic skeletal muscle, Mol. Ther. 5 (3) (2002) 300–306, https://doi.org/10.1006/mthe.2002.0539.

[26] J.M. Morais, F. Papadimitrakopoulos, D.J. Burgess, Biomaterials/tissue interactions: possible solutions to overcome foreign body response, AAPS J. 12 (2) (2010) 188–196, https://doi.org/10.1208/s12248-010-9175-3.

[27] A. Assmann, C. Delfs, H. Munakata, F. Schiffer, K. Horstkötter, K. Huynh, M. Barth, V.R. Stoldt, H. Kamiya, U. Boeken, Acceleration of autologous in vivo recellularization of decellularized aortic conduits by fibronectin surface coating, Biomaterials 34 (25) (2013) 6015–6026, https://doi.org/10.1016/j.biomaterials.2013.04.037.

[28] M. Shafiq, Q. Zhang, D. Zhi, K. Wang, D. Kong, D.H. Kim, S.H. Kim, In situ blood vessel regeneration using SP (substance P) and SDF (stromal cell-derived factor)-1 alpha peptide eluting vascular grafts, Arterioscler. Thromb. Vasc. Biol. 38 (7) (2018) e117–e134, https://doi.org/10.1161/atvbaha.118.310934.

[29] W. Zeng, C. Wen, Y. Wu, L. Li, Z. Zhou, J. Mi, W. Chen, M. Yang, C. Hou, J. Sun, The use of BDNF to enhance the patency rate of small-diameter tissue-engineered blood vessels through stem cell homing mechanisms, Biomaterials 33 (2) (2012) 473–484, https://doi.org/10.1016/j.biomaterials.2011.09.066.

[30] M. Shafiq, Y. Jung, S.H. Kim, Covalent immobilization of stem cell inducing/recruiting factor and heparin on cell-free small-diameter vascular graft for accelerated in situ tissue regeneration, J. Biomed. Mater. Res. 104 (6) (2016) 1352–1371, https://doi.org/10.1002/jbm.a.35666.

[31] M.T. Koobatian, S. Row, R.J. Smith Jr., C. Koenigsknecht, S.T. Andreadis, D.D. Swartz, Successful endothelialization and remodeling of a cell-free small-diameter arterial graft in a large animal model, Biomaterials 76 (2016) 344–358, https://doi.org/10.1016/j.biomaterials.2015.10.020.

[32] M. Shafiq, S.-H. Lee, Y. Jung, S. Hyun Kim, Strategies for recruitment of stem cells to treat myocardial infarction, Curr. Pharmaceut. Des. 21 (12) (2015) 1584–1597, https://doi.org/10.2174/1381612821666150115151938.

[33] T. Liu, Y. Wang, W. Zhong, B. Li, K. Mequanint, G. Luo, M.A.-O. Xing, Biomedical Applications of Layer-By-Layer Self-Assembly for Cell Encapsulation: Current Status and Future Perspectives, 2192-2659 (Electronic)) https://doi.org/10.1002/adhm.201800939.

[34] L.M. Ojemann, W.L. Nelson, D.S. Shin, A.O. Rowe, R.A. Buchanan, Tian ma, an ancient Chinese herb, offers new options for the treatment of epilepsy and other conditions, Epilepsy Behav. 8 (2) (2006) 376–383, https://doi.org/10.1016/j.yebeh.2005.12.009.

[35] Q. Zhang, Y.-m. Yang, G.-y. Yu, [Effects of gastrodin injection on blood pressure and vasoactive substances in treatment of old patients with refractory hypertension: a randomized controlled trial], Zhong Xi Yi Jie He Xue Bao 6 (7) (2008) 695–699, https://doi.org/10.3736/jcim20080707.

[36] X. Zeng, S. Zhang, L. Zhang, K. Zhang, X. Zheng, A study of the neuroprotective effect of the phenolic glucoside gastrodin during cerebral ischemia in vivo and in vitro, Planta Med. 72 (15) (2006) 1359–1365, https://doi.org/10.1055/s-2006-951709.

[37] Y. Liu, X. Tang, J. Pei, L. Zhang, F. Liu, K. Li, Gastrodin interaction with human fibrinogen: anticoagulant effects and binding studies, Chemistry 12 (30) (2006) 7807–7815, https://doi.org/10.1002/chem.200600549.

[38] H. Wang, R. Zhang, Y. Qiao, F. Xue, H. Nie, Z. Zhang, Y. Wang, Z. Peng, Q. Tan, Gastrodin ameliorates depression-like behaviors and up-regulates proliferation of hippocampal-derived neural stem cells in rats: involvement of its anti-inflammatory action, Behav. Brain Res. 266 (2014) 153–160, https://doi.org/10.1016/j.bbr.2014.02.046.

[39] Z. Peng, S. Wang, G. Chen, R. Liu, J. Deng, J. Liu, T. Zhang, Q. Tan, C. Hai, Gastrodin alleviates cerebral ischemic damage in mice by improving anti-oxidant and anti-inflammation activities and inhibiting apoptosis pathway, Neurochem. Res. 40 (4) (2015) 661–673, https://doi.org/10.1007/s11064-015-1513-5.

[40] X. Zeng, S. Zhang, L. Zhang, K. Zhang, X. Zheng, A study of the neuroprotective effect of the phenolic glucoside gastrodin during cerebral ischemia in vivo and in vitro, Planta Med. 72 (15) (2007) 1359–1365, https://doi.org/10.1055/s-2006-951709.

[41] L. Li, Q. Li, J. Yang, L. Sun, J. Guo, Y. Yao, L. Zhong, D. Lu, Enhancement in mechanical properties and cell activity of polyurethane scaffold derived from gastrodin, Mater. Lett. 228 (2018) 435–438, https://doi.org/10.1016/j.matlet.2018.06.061.

[42] Z. Ma, Y. Hong, D.M. Nelson, J.E. Pichamuthu, C.E. Leeson, W.R. Wagner, Biodegradable polyurethane ureas with variable polyester or polycarbonate soft segments: effects of crystallinity, molecular weight, and composition on mechanical properties, Biomacromolecules 12 (9) (2011) 3265–3274, https://doi.org/10.1021/bm2007218.

[43] N. Koupaei, A. Karkhaneh, M. Daliri Joupari, Preparation and characterization of (PCL-crosslinked-PEG)/hydroxyapatite as bone tissue engineering scaffolds, J. Biomed. Mater. Res. 103 (12) (2015) 3919–3926, https://doi.org/10.1002/jbm.a.35513.

[44] S. Asadpour, H. Yeganeh, J. Ai, S. Kargozar, M. Rashtbar, A. Seifalian, H. Ghanbari, Polyurethane-Polycaprolactone blend patches: scaffold characterization and cardiomyoblast adhesion, proliferation, and function, Acs Biomater. Sci. Eng. (2018), https://doi.org/10.1021/acsbiomaterials.8b00848.

[45] H.F. Naguib, M.S.A. Aziz, S.M. Sherif, G.R. Saad, Synthesis and thermal characterization of poly (ester-ether urethane) s based on PHB and PCL-PEG-PCL blocks, J. Polym. Res. 18 (5) (2011) 1217–1227, https://doi.org/10.1007/s10965-010-9525-y.

[46] S. Zhou, X. Deng, H. Yang, Biodegradable poly(epsilon-caprolactone)-poly(ethylene glycol) block copolymers: characterization and their use as drug carriers for a controlled delivery system, Biomaterials 24 (20) (2003) 3563–3570, https://doi.org/10.1016/s0142-9612(03)00207-2.

[47] D. de Cassan, S. Sydow, N. Schmidt, P. Behrens, Y. Roger, A. Hoffmann, A.L. Hoheisel, B. Glasmacher, R.H. nsch, H. Menzel, Attachment of nanoparticulate drug-release systems on poly(ε-caprolactone) nanofibers via a graftpolymer as interlayer, Colloids Surf. B Biointerfaces 163 (2018) 309–320, https://doi.org/10.1016/j.colsurfb.2017.12.050 S0927776517308901.

[48] U. Makal, N. Uslu, K.J. Wynne, Water makes it hydrophobic: contraphilic wetting for polyurethanes with soft blocks having semifluorinated and 5,5-dimethylhydantoin side chains, Langmuir 23 (1) (2007) 209–216, https://doi.org/10.1021/la0615600.

[49] M.A. Javaid, R.A. Khera, K.M. Zia, K. Saito, I.A. Bhatti, M. Asghar, Synthesis and characterization of chitosan modified polyurethane bio-nanocomposites with biomedical potential, Int. J. Biol. Macromol. 115 (2018) 375–384, https://doi.org/10.1016/j.ijbiomac.2018.04.013 S0141813018309115.

[50] N.I. Baek, S.Y. Choi, J.K. Park, S.W. Cho, E.M. Ahn, S.G. Jeon, B.R. Lee, J.H. Bahn, Y.K. Kim, I.H. Shon, Isolation and identification of succinic semialdehyde dehydrogenase inhibitory compound from the rhizome of Gastrodia elata Blume, Arch Pharm. Res. (Seoul) 22 (2) (1999) 219–224, https://doi.org/10.1007/bf02976550.

[51] D. Dutta, K.W. Lee, R.A. Allen, Y. Wang, J.C. Brigham, K. Kim, Non-invasive assessment of elastic modulus of arterial constructs during cell culture using ultrasound elasticity imaging, Ultrasound Med. Biol. 39 (11) (2013) 2103–2115, https://doi.org/10.1016/j.ultrasmedbio.2013.04.023.

[52] K.J. Pawlowski, S.E. Rittgers, S.P. Schmidt, G.L. Bowlin, Endothelial cell seeding of polymeric vascular grafts, Front. Biosci. 9 (2004) 1412–1421, https://doi.org/10.2741/1302.

[53] L. Soletti, A. Nieponice, Y. Hong, S.H. Ye, J.J. Stankus, W.R. Wagner, D.A. Vorp, In vivo performance of a phospholipid-coated bioerodable elastomeric graft for small-diameter vascular applications, J. Biomed. Mater. Res. 96 (2) (2011) 436–448, https://doi.org/10.1002/jbm.a.32997.

[54] W. Wu, R.A. Allen, Y. Wang, Fast-degrading elastomer enables rapid remodeling of a cell-free synthetic graft into a neoartery, Nat. Med. 18 (7) (2012) 1148–1153, https://doi.org/10.1038/nm.2821.

[55] P.H. Blit, W.G. McClung, J.L. Brash, K.A. Woodhouse, J.P. Santerre, Platelet inhibition and endothelial cell adhesion on elastin-like polypeptide surface modified materials, Biomaterials 32 (25) (2011) 5790–5800, https://doi.org/10.1016/j.biomaterials.2011.04.067.

[56] Y. Hong, S.H. Ye, A. Nieponice, L. Soletti, D.A. Vorp, W.R. Wagner, A small diameter, fibrous vascular conduit generated from a poly(ester urethane)urea and phospholipid polymer blend, Biomaterials 30 (13) (2009) 2457–2467, https://doi.org/10.1016/j.biomaterials.2009.01.013.

[57] H.W. Jun, L.J. Taite, J.L. West, Nitric oxide-producing polyurethanes, Biomacromolecules 6 (2) (2005) 838–844, https://doi.org/10.1021/bm049419y.

[58] E.A. Lipke, J.L. West, Localized delivery of nitric oxide from hydrogels inhibits neointima formation in a rat carotid balloon injury model, Acta Biomater. 1 (6) (2005) 597–606, https://doi.org/10.1016/j.actbio.2005.07.010.

[59] L.J. Taite, P. Yang, H.W. Jun, J.L. West, Nitric oxide-releasing polyurethane-PEG copolymer containing the YIGSR peptide promotes endothelialization with decreased platelet adhesion, J. Biomed. Mater. Res. B Appl. Biomater. 84 (1) (2008) 108–116, https://doi.org/10.1002/jbm.b.30850.

[60] C. Del Gaudio, E. Ercolani, P. Galloni, F. Santilli, S. Baiguera, L. Polizzi, A. Bianco, Aspirin-loaded electrospun poly(ε-caprolactone) tubular scaffolds: potential small-diameter vascular grafts for thrombosis prevention, J. Mater. Sci. Mater. Med. 24 (2) (2013) 523–532, https://doi.org/10.1007/s10856-012-4803-3.

[61] F. Innocente, D. Mandracchia, E. Pektok, B. Nottelet, J.C. Tille, S. de Valence, G. Faggian, A. Mazzucco, A. Kalangos, R. Gurny, M. Moeller, B.H. Walpoth, Paclitaxel-eluting biodegradable synthetic vascular prostheses: a step towards reduction of neointima formation? Circulation 120 (11 Suppl) (2009) S37–S45, https://doi.org/10.1161/CIRCULATIONAHA.109.848242.

[62] E.M. Christenson, J.M. Anderson, A. Hiltner, Biodegradation mechanisms of polyurethane elastomers, Br. Corrosion J. 42 (4) (2015) 312–323, https://doi.org/10.1179/174327807X238909.

[63] R.J. Zdrahala, I.J. Zdrahala, Biomedical Applications of polyurethanes: a review of past promises, present realities, and a vibrant future, J. Biomater. Appl. 14 (1) (1999) 67–90, https://doi.org/10.1177/088532829901400104.

[64] M. Kütting, J. Roggenkamp, U. Urban, T. Schmitz-Rode, U. Steinseifer, Polyurethane heart valves: past, present and future, Expet Rev. Med. Dev. 8 (2) (2011), https://doi.org/10.1586/erd.10.79 277-233.

[65] P. Punnakitikashem, D. Truong, J.U. Menon, K.T. Nguyen, Y. Hong, Electrospun biodegradable elastic polyurethane scaffolds with dipyridamole release for small diameter vascular grafts, Acta Biomater. 10 (11) (2014) 4618–4628, https://doi.org/10.1016/j.actbio.2014.07.031.
[66] D. Druecke, S. Langer, E. Lamme, J. Pieper, M. Ugarkovic, H.U. Steinau, H.H. Homann, Neovascularization of poly(ether ester) block-copolymer scaffolds in vivo: long-term investigations using intravital fluorescent microscopy, J. Biomed. Mater. Res. 68A (1) (2004), https://doi.org/10.1002/jbm.a.20016.
[67] J.Y. Zhang, E.J. Beckman, J. Hu, G.G. Yang, S. Agarwal, J.O. Hollinger, Synthesis, Biodegradability, and biocompatibility of lysine diisocyanate–glucose polymers, Tissue Eng. 8 (5) (2002) 771–785, https://doi.org/10.1089/10763270260424132.
[68] L. Yang, J. Li, S. Meng, Y. Jin, J. Zhang, M. Li, J. Guo, Z. Gu, The in?vitro and in?vivo degradation behavior of poly (trimethylene carbonate-co-ε-caprolactone) implants, Polymer 55 (20) (2014) 5111–5124, https://doi.org/10.1016/j.polymer.2014.08.027.
[69] F. Shokrolahi, H. Yeganeh, Soft segment composition and its influence on phase-separated morphology of PCL/PEG-based poly(urethane urea)s, Iran. Polym. J. (Engl. Ed.) 23 (7) (2014) 505–512, https://doi.org/10.1007/s13726-014-0245-8.
[70] S.Y. Lee, S.C. Wu, H. Chen, L.L. Tsai, J.J. Tzeng, C.H. Lin, Y.M. Lin, Synthesis and characterization of polycaprolactone-based polyurethanes for the fabrication of elastic guided bone regeneration membrane, BioMed Res. Int. (2018) 3240571, https://doi.org/10.1155/2018/3240571.
[71] P.W. Raut, A.A. Shitole, A. Khandwekar, N. Sharma, Engineering biomimetic polyurethane using polyethylene glycol and gelatin for blood-contacting applications, J. Mater. Sci. 54 (2019) 10457–10472, https://doi.org/10.1007/s10853-019-03643-0.
[72] H.L. Jin, W.L. Jin, G. Khang, B.L. Hai, Interaction of cells on chargeable functional group gradient surfaces, Biomaterials 18 (4) (1997) 351–358, https://doi.org/10.1016/S0142-9612(96)00128-7.
[73] H.L. Jin, J.L. Sang, G. Khang, B.L. Hai, The effect of fluid shear stress on endothelial cell adhesiveness to polymer surfaces with wettability gradient, J. Colloid Interface Sci. 230 (1) (2000) 84–90, https://doi.org/10.1006/jcis.2000.7080.
[74] P.B.V. Wachem, A.H. Hogt, T. Beugeling, J. Feijen, A. Bantjes, J.P. Detmers, W.G.V. Aken, Adhesion of cultured human endothelial cells onto methacrylate polymers with varying surface wettability and charge, Biomaterials 8 (5) (1987) 323–328, https://doi.org/10.1016/0142- 9612(87)90001-9.
[75] Y. Tamada, Y. Ikada, Effect of preadsorbed proteins on cell adhesion to polymer surfaces, J. Colloid Interface Sci. 155 (2) (1993) 334–339, https://doi.org/10.1006/jcis.1993.1044.
[76] Y. Tamada, Y. Ikada, Fibroblast growth on polymer surfaces and biosynthesis of collagen, J. Biomed. Mater. Res. 28 (7) (1994) 783–789, https://doi.org/10.1002/jbm.820280705.
[77] H.L. Jin, B.L. Hai, A wettability gradient as a tool to study protein adsorption and cell adhesion on polymer surfaces, J. Biomater. Sci. Polym. Ed. 4 (5) (1993) 467–481, https://doi.org/10.1163/156856293X00131.
[78] V.M. Merkle, D. Martin, M. Hutchinson, P.L. Tran, A. Behrens, S. Hossainy, J. Sheriff, D. Bluestein, X. Wu, M.J. Slepian, Hemocompatibility of poly(vinyl alcohol)-gelatin core-shell electrospun nanofibers: a scaffold for modulating platelet deposition and activation, ACS Appl. Mater. Interfaces 7 (15) (2015) 8302–8312, https://doi.org/10.1021/acsami.5b01671.
[79] I. Firkowska-Boden, X. Zhang, K.D. Jandt, Controlling protein adsorption through nanostructured polymeric surfaces, Adv Healthc Mater 7 (1) (2018), https://doi.org/10.1002/adhm.201700995.
[80] Q. Yang, S. Liu, X. Liu, Z. Liu, W. Xue, Y. Zhang, Role of charge-reversal in the hemo/immuno-compatibility of polycationic gene delivery systems, Acta Biomater. 96 (2019) 436–455, https://doi.org/10.1016/j.actbio.2019.06.043.
[81] H. Wang, Y. Feng, Z. Fang, W. Yuan, M. Khan, Co-electrospun blends of PU and PEG as potential biocompatible scaffolds for small-diameter vascular tissue engineering, Mater. Sci. Eng. C 32 (8) (2012) 2306–2315, https://doi.org/10.1016/j.msec.2012.07.001.
[82] Motlagh Delara, Yang Jian, Y. Lui Karen, Hemocompatibility evaluation of poly (glycerol-Sebacate) in vitro for vascular tissue engineering, Biomaterials (2006), https://doi.org/10.1016/j.biomaterials.2006.04.010.
[83] N.V. Efremova, S.R. Sheth, D.E. Leckband, Protein-induced changes in poly (ethylene glycol) brushes: molecular weight and temperature dependence, Langmuir 17 (24) (2001) 7628–7636, https://doi.org/10.1021/la010405c.
[84] T. Mcpherson, A. Kidane, I. Szleifer, K. Park, Prevention of protein adsorption by tethered poly(ethylene oxide) layers: experiments and single-chain mean-field analysis, Langmuir 14 (1) (1998), https://doi.org/10.1021/la9706781.
[85] S. Li, Z. Guo, Y. Zhang, W. Xue, Z. Liu, Blood compatibility evaluations of fluorescent carbon dots, ACS Appl. Mater. Interfaces 7 (34) (2015), https://doi.org/10.1021/acsami.5b04866 150819071118009.
[86] G. Strandberg, M. Lipcsey, M. Eriksson, N. Lubenow, A. Larsson, Analysis of thromboelastography, PT, APTT and fibrinogen in intraosseous and venous samples-an experimental study, Scand J Trauma Resusc Emerg Med 24 (1) (2016) 131, https://doi.org/10.1186/s13049-016-0318-0.
[87] J. Lin, Y. Shi, J. Miao, Y. Wu, H. Lin, J. Wu, W. Zeng, F. Qi, C. Liu, X. Wang, Gastrodin alleviates oxidative stress-induced apoptosis and cellular dysfunction in human umbilical vein endothelial cells via the nuclear factor-erythroid 2-related factor 2/heme oxygenase-1 pathway and accelerates wound healing in vivo, Front. Pharmacol. 10 (2019) 1273, https://doi.org/10.3389/fphar.2019.01273.
[88] J.M. Anderson, A. Rodriguez, D.T. Chang, Foreign body reaction to biomaterials, Semin. Immunol. 20 (2) (2008) 100, https://doi.org/10.1016/j.smim.2007.11.004.
[89] D.F. Williams, S.P. Zhong, Talking point. Are free radicals involved in biodegradation of implanted polymers? Adv. Mater. 3 (12) (2004) 623–626, https://doi.org/10.1002/adma.19910031213.
[90] P. Niethammer, C. Grabher, A.T. Look, T.J. Mitchison, A tissue-scale gradient of hydrogen peroxide mediates rapid wound detection in zebrafish, Nature 459 (7249) (2009) 996–999, https://doi.org/10.1038/nature08119.
[91] R.P. Juni, H.J. Duckers, P.M. Vanhoutte, R. Virmani, A.L. Moens, Oxidative stress and pathological changes after coronary artery interventions, J. Am. Coll. Cardiol. 61 (14) (2013) 1471, https://doi.org/10.1016/j.jacc.2012.11.068.
[92] Zhang Hongbin, Yuan Bo, Huang Hanfei, Qu Siming, Yang Shikun, Gastrodin induced HO-1 and Nrf2 up-regulation to alleviate H2O2-induced oxidative stress in mouse liver sinusoidal endothelial cells through p38 MAPK phosphorylation, Revista Brasileira De Pesquisas Medicas E Biologicas (2018), https://doi.org/10.1590/1414-431x20187439.
[93] C. Wang, B. Chen, W. Wang, X. Zhang, T. Hu, Y. He, K. Lin, X. Liu, Strontium released bi-lineage scaffolds with immunomodulatory properties induce a pro-regenerative environment for osteochondral regeneration, Mater. Sci. Eng. C 103 (2019) 109833, https://doi.org/10.1016/j.msec.2019.109833.
[94] J.M. Sadowska, F. Wei, J. Guo, J. Guillem-Marti, Y. Xiao, The effect of biomimetic calcium deficient hydroxyapatite and sintered β-tricalcium phosphate on osteoimmune reaction and osteogenesis, Acta Biomater. 96 (2019), https://doi.org/10.1016/j.actbio.2019.06.057.
[95] C.T. Esmon, Reprint of Crosstalk between inflammation and thrombosis, Maturitas 61 (1–2) (2008) 122–131, https://doi.org/10.1016/j.maturitas.2008.11.008.
[96] M. Levi, H.T. Cate, Current concepts - disseminated intravascular coagulation, N. Engl. J. Med. 341 (8) (1999) 586–592, https://doi.org/10.1056/NEJM199908193410807.
[97] A.T. Nurden, Platelets, inflammation and tissue regeneration, Thromb. Haemostasis 105 (Suppl 1) (2011) S13–S33, https://doi.org/10.1160/ths10-11-0720.
[98] P. Yang, Y. Han, L. Gui, J. Sun, L. Sun, Gastrodin attenuation of the inflammatory response in H9c2 cardiomyocytes involves inhibition of NF-κB and MAPKs activation via the phosphatidylinositol 3-kinase signaling, Biochem. Pharmacol. 85 (8) (2013), https://doi.org/10.1016/j.bcp.2013.01.020.
[99] M.A. Schwartz, D. Vestweber, M. Simons, A unifying concept in vascular health and disease, Science 360 (6386) (2018) 270–271, https://doi.org/10.1126/science.aat3470.
[100] E.B. Peters, Endothelial progenitor cells for the vascularization of engineered tissues, Tissue Eng Part B Rev 24 (1) (2017) 1–24, https://doi.org/10.1089/ten.TEB.2017.0127.
[101] C. Vyas, R. Pereira, B. Huang, F. Liu, W. Wang, P. Bartolo, Engineering the vasculature with additive manufacturing, Curr. Opn. Biomed. Eng. 2 (2017) 1–13, https://doi.org/10.1016/j.cobme.2017.05.008.
[102] J. Lin, Y. Shi, J. Miao, Y. Wu, H. Lin, J. Wu, W. Zeng, F. Qi, C. Liu, X. Wang, H. Jin, Gastrodin alleviates oxidative stress-induced apoptosis and cellular dysfunction in human umbilical vein endothelial cells via the nuclear factor-erythroid 2-related factor 2/heme oxygenase-1 pathway and accelerates wound healing in vivo, Front. Pharmacol. 10 (2019) 1273, https://doi.org/10.3389/fphar.2019.01273.
[103] O.F. Khan, M.V. Sefton, Endothelialized biomaterials for tissue engineering applications in vivo, Trends Biotechnol. 29 (8) (2011) 379–387, https://doi.org/10.1016/j.tibtech.2011.03.004.